

1 **Effect of fine recycled concrete aggregate on the mechanical behavior of self-**
2 **compacting concrete**

3 Víctor Revilla-Cuesta^{a*}, Vanesa Ortega-López^a, Marta Skaf^b and Juan Manuel Manso^a

4 ^a Affiliation: Department of Civil Engineering. University of Burgos, Spain.

5 Address: EPS. Calle Villadiego s/n. 09001 Burgos. Spain.

6 Emails: vrevilla@ubu.es; vortega@ubu.es; jmmanso@ubu.es

7

8 ^b Affiliation: Department of Construction. University of Burgos, Spain.

9 Address: EPS. Calle Villadiego s/n. 09001 Burgos. Spain.

10 Email: mskaf@ubu.es

11

12 ***Corresponding Author:**

13 Víctor Revilla-Cuesta

14 Department of Civil Engineering, University of Burgos.

15 Escuela Politécnica Superior. Calle Villadiego s/n, 09001 Burgos, Spain.

16 Phone: +34947497117

17 e-mail: vrevilla@ubu.es

18 **Abstract**

19 The high flowability of Self-Compacting Concrete (SCC) is achieved by adding large amounts of fine
20 aggregate. Therefore, the addition of fine Recycled Concrete Aggregate (RCA) in this type of concrete
21 can very noticeably change its behavior. SCCs with different percentages of fine RCA (0 %, 25 %, 50 %,
22 75 %, and 100 %) and 100 % coarse RCA were manufactured in this study, to evaluate their
23 performance, and to analyze the effect of fine RCA in an SCC when a high amount of coarse RCA is also
24 added. Both the fresh properties (flowability, density, and air content) and their mechanical behavior
25 (strengths, non-destructive tests, stress-strain curves, and Poisson coefficient) at different curing ages
26 were studied. These mechanical properties were compared with the values calculated using the
27 formulas from two of the most common structural design standards. High values of strength and
28 modulus of elasticity were obtained up to a fine RCA content of 50 %. Additionally, any increase in fine
29 RCA increased flowability and elastic and plastic deformability of the SCC. The theoretical values
30 overestimated the experimental ones by around 25 %. From the mechanical point of view, SCC with
31 up to 50 % fine RCA could be used for structural applications, although service requirements regarding
32 deformability recommend that its content should be limited to 25 %.

33 **Keywords:** Self-Compacting Concrete; Recycled Concrete Aggregate; flowability; mechanical
34 performance at different curing ages; stress-strain curves; design values

35 1. Introduction

36 Construction sector activities are generally characterized as large-scale projects that consume vast
37 amounts of natural resources, something that the production figures of the sector largely reflect. On
38 average, within the European Union, around 2,700 Mt of Natural Aggregate (NA) are placed on the
39 market each year, of which 120 million were consumed in Spain. Moreover, 16 Mt of bituminous
40 concrete, and 22 Mm³ of hydraulic concrete were produced, in 2018, in this country [1]. High levels of
41 resource exploitation have continued over time, leading in some areas to significant scarcities [2].

42 Construction and Demolition Waste (CDW) represents 34.7 % of all building waste generated in
43 Europe, over 800 Mt/year, where the countries with the highest production levels are France and
44 Germany (227 and 207 Mt/year respectively) [3]. In Spain, with the upturn of the construction sector,
45 CDW production exceeded 20 Mt in 2017 [3]. Demolition processes generated around 0.9 t of CDW
46 per m² of demolished housing, reaching 1.2 t/m² in industrial buildings, 40 % of which was deposited
47 in illegal landfill sites [4]. CDWs usually present a mixture of concrete with ceramic residues and glass
48 and/or gypsum, which worsen their behavior as a raw material for other uses [5]. Recycled Concrete
49 Aggregate (RCA), a particular type of CDW, is usually produced from the crushing of selected concrete
50 elements, such as precast concrete rejects, and it demonstrates better mechanical behavior, because
51 it contains fewer contaminants and its properties are less variable [6].

52 The two above-mentioned problems -scarcity of natural resources and abundance of waste- could be
53 mitigated through a simple strategy: using waste as a raw material in different construction sector
54 applications, in substitution of NA, among which the manufacture of hydraulic and bituminous
55 concretes is notable [7-13]. This strategy would also help to reduce the ecological impact of quarrying
56 as well as the carbon footprint of the construction sector [5; 14-16]. Among the various potential
57 usages of RCA, this study is focused on its validation in the manufacture of Self-Compacting Concrete
58 (SCC).

59 The total aggregate volume of concrete is 65-70 %, making RCA an ideal material for applying the above
60 strategy. In fact, the literature contains several studies of conventional concretes made with proper
61 dosages of coarse RCA that have demonstrated a good behavior [17; 18]. The addition of fine RCA has
62 a more harmful effect, causing a very noticeable decrease in the mechanical properties of the
63 concretes in which it is incorporated [19]. Although there are some studies on high-performance
64 concretes, such as SCC [20], the available bibliography is scarce, fundamentally in relation to fine RCA,
65 a remarkable aspect, considering the importance of the fine aggregate fractions within this type of
66 concrete [21].

67 The aspects commented on above are due to the particular characteristics of RCA. The coarse fraction
68 of RCA, which is larger than 4 mm, is mainly characterized by three interrelated aspects. Firstly, the
69 mortar adhering to the surface of the RCA means that, in comparison with the NA, its density and
70 hardness are lower [22; 23]. Secondly, RCA has a contact surface between the aggregate and the
71 mortar, known as the Interfacial Transition Zone (ITZ) [24], which is weaker and less dense than the
72 ITZ of NA [22; 25]. Finally, the high water absorption levels of RCA can be due to the unhydrated cement
73 in the attached mortar [23; 25]. The behavior of the fine RCA, less than 4 mm in size, is strongly
74 conditioned by the mortar particles, as well as some pollutants (clay, gypsum and mica), mainly
75 introduced during the crushing process, which cause, among other aspects, higher levels of water
76 absorption than in the coarse fraction [26].

77 The addition of RCA affects not only both the fresh and the hardened behavior of the concrete, but
78 also the estimation of compressive strength through non-destructive testing, such as the hammer
79 rebound index and Ultrasonic Pulse Velocity (UPV), mainly due to the presence of attached mortar
80 [27]. However, the validity of these procedures has been demonstrated in vibrated concrete with high
81 contents of coarse RCA [28; 29], even at early ages [30]. Despite the low coarse aggregate content of
82 SCC, non-destructive tests are also valid for this type of concrete when NA is used [31].

83 The aim of this study is to evaluate the effect of adding different amounts of fine RCA in an SCC with a
84 constant amount of coarse RCA. SCC requires a high proportion of fine aggregate to reach flowability,
85 so it is more sensitive to the effects of fine RCA. In addition, the interaction between coarse and fine
86 RCA can influence its performance. The coarse RCA content was defined in a preliminary analysis,
87 involving tests on the compressive strengths and the elastic moduli of mixes with 0 %, 50 % and 100 %
88 of coarse RCA. Based on this analysis, the amount of 100 % coarse RCA was chosen for the optimum
89 sustainability of the product. Subsequently, five different SCCs with 100 % coarse RCA and fine RCA
90 percentages of 0 %, 25 %, 50 %, 75 % and 100 % were manufactured and analyzed in this study.

91 Firstly, the evaluation of the fresh concrete behavior of these SCCs verified their compliance with all
92 the recommendations of the European Federation of National Associations Representing producers
93 and applicators of specialist building products for Concrete (EFNARC) [32]. Subsequently, the temporal
94 evolution of the mechanical properties was evaluated. Additionally, the theoretical values of these
95 mechanical properties, estimated from their compressive strengths, were calculated and compared
96 with the experimental values, in order to validate the calculation methods. The validity of RCA as a
97 material for manufacturing SCC for structural usage was therefore demonstrated, in accordance with
98 its dosage (in particular, the percentage of fine RCA), which must be selected to meet the main purpose
99 of the concrete design (self-compactability and/or strength).

100 **2. Materials**

101 The characteristics of the materials used in this study are described in this section. An analysis of the
102 physical properties and the chemical composition of the RCA is also included, to evaluate its suitability
103 for concrete manufacture.

104 **2.1. Cement, water, filler and admixtures**

105 A conventional Portland cement CEM I 52.5 R was used, with a density of 3.12 Mg/m^3 and a clinker
106 content of around 98 %. Mix water that contained no chemical compounds with potentially adverse
107 effects on concrete behavior was taken from the water supply of the city of Burgos, Spain.

108 The finest fraction of the granulometry ($< 0.063 \text{ mm}$) was provided by the addition of limestone filler
109 with a CaCO_3 content higher than 98 %. According to the manufacturer's specifications, this filler had
110 a density of 2.77 Mg/m^3 and a water absorption rate of 0.54 % over 24 h (0.37 % in 10 minutes).

111 Two additives, fundamental components for providing the SCC with its characteristic self-
112 compactability, were used, which had demonstrated good behavior in a similar study [33]. The first
113 one, a plasticizer, enhanced concrete flowability. The second, a viscosity regulator, maintained SCC
114 flowability over longer periods, improving the results of the in-fresh state tests. In all dosages, total
115 additions of admixture amounted to 2.2 % by weight of cement.

116 **2.2. Aggregates (RCA, siliceous gravel and siliceous sand)**

117 The RCA was produced from concrete components with a characteristic strength of 45 MPa,
118 manufactured with siliceous aggregate, which had subsequently been rejected by the prefabrication
119 industry and crushed. Supplied in sizes between 0 and 31.5 mm from a local CDW management
120 company, the RCA was sieved and separated into fine RCA (0/4 mm) and coarse RCA (4/12.5 mm)
121 fractions, both of which were used in this study.

122 In Table 1, the main properties of the RCA are compared with the recommended limit values from the
123 Spanish concrete standard EHE-08 [34]. The comparison shows that the RCA fulfilled most of the
124 requirements, except for density and water absorption, which explains the limitation that is specified
125 in the standard of a maximum content of 20 % total coarse RCA. The chemical composition of fine RCA
126 obtained by X-ray fluorescence (XRF) spectrometry and the X-ray diffraction (XRD) pattern are shown
127 in Table 2 and Figure 1, respectively. The predominance of silicon oxide and calcium carbonate can be
128 observed in its composition. The hydrated cementitious components (CSH) are not visible in the XRD
129 test results, although the content in both aluminum and iron oxides denotes the presence of old
130 mortar in the fine RCA.

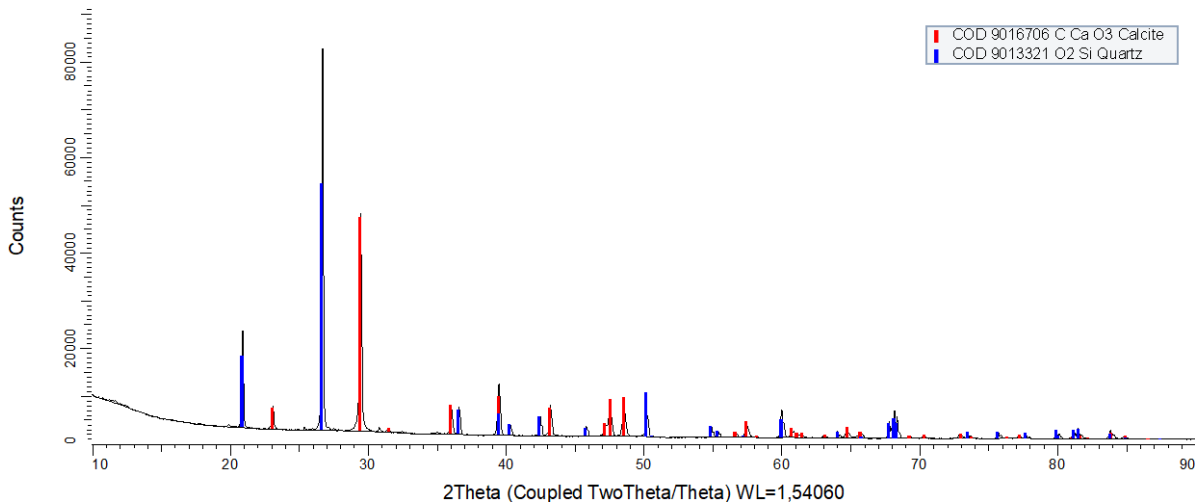
131 Siliceous gravel and sand were used to complete the coarse (preliminary analysis) and the fine
 132 aggregate fraction of each concrete mix. Their properties are also summarized in Table 1.

Test	Regulations [35]	Siliceous gravel	Siliceous sand	Coarse RCA	Fine RCA	EHE-08 limit [34]
Saturated-Surface-Dry (SSD) density (Mg/m ³)	EN-1097-6	2.62	2.58	2.42	2.37	≈ 2.6 kg/dm ³
Water absorption 24h (%)	EN-1097-6	0.84	0.25	6.25	7.36	Coarse RCA content < 20 %: <7 % Coarse RCA content > 20 %: Combination of RCA and NA coarse fractions: < 5 %
Water absorption 10 minutes (%)	-	0.66	0.18	5.28	6.03	If RCA content is lower than 20 %: <5.5 %
Fines content (%)	EN-933-1	0.11	1.82	0.17	4.83	< 1.50 % (coarse fraction)
Equivalent sand (%)	EN-933-8	-	-	-	83	> 75
Bulk density (Mg/m ³)	EN-1097-3	-	-	1.26	1.23	-
Los Angeles coefficient (%) (size 10/14 mm)	EN-1097-2	-	-	35	-	< 40
Sand friability test (%) (size 0/4 mm)	UNE-146404	-	-	-	16	

133 Table 1. Aggregates' physical properties.

SiO ₂	CaO	Al ₂ O ₃	Fe ₂ O ₃	SO ₃	MgO	K ₂ O	TiO ₂	P ₂ O ₅	Others (CO ₂ ...)
50.80	20.00	3.74	1.12	1.00	0.63	0.60	0.15	0.06	21.9

134 Table 2. Chemical composition (% in weight) of fine RCA trough XRF.



135
 136 Figure 1. XRD of fine RCA

137 The granulometric curves of all aggregates are shown in Figure 2. It can be seen that the fine RCA
 138 shows higher percentages of fine particles than the siliceous sand.

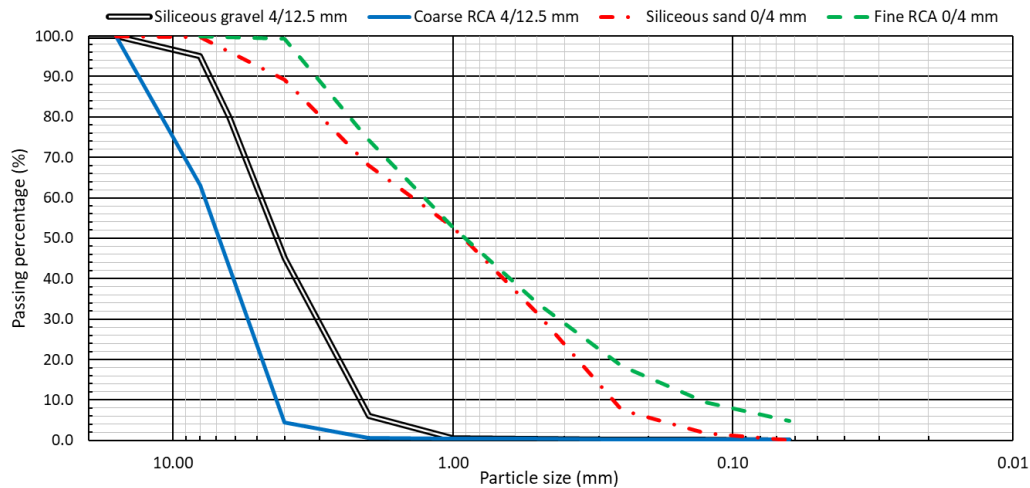


Figure 2. Granulometry of aggregates used

139
140
141

3. Methodology

142 In this section, the design of the experiment is explained. Firstly, a preliminary analysis is shown to
143 define the coarse RCA content in the mixes. Secondly, the dosage of the SCCs with different
144 percentages of fine RCA are defined. Thirdly, the set of tests performed on the mixes is discussed.
145 Finally, the type of analysis of the experimental data is likewise explained.

3.1. Experiment design

147 Firstly, a preliminary analysis served to define the amount of coarse RCA to use in the mixes. Based on
148 this analysis, it was decided to use 100 % coarse RCA (see section 3.2). Later, the fine RCA contents
149 (25 %, 50 %, 75 % and 100 %), the set of tests to carry out and the number of samples in each test
150 (application of the power method, with a significance level of 5 % and a power of 20 %) was defined
151 by analyzing other similar research studies [36; 37]. In addition, testing ages were established
152 according to the standards [34; 38; 39], in order to evaluate the effect of fine RCA over time. Therefore,
153 age and fine RCA content were the two factors evaluated in this study.

3.2. Mix design

155 The dosage of all mixes was defined by the specifications of EHE-08 [34], based on EC2 [39]. The overall
156 particle size was adjusted to the Fuller curve, using the granulometric modules of the aggregates.
157 Rather than the addition of admixtures to the mix design, the water content in the mixtures was
158 carefully increased to achieve a proper self-compactability. That decision was taken to avoid admixture
159 segregation that occurred when its proportion in the mix exceeded 2.2 % of cement mass.

160 **3.2.1. Preliminary analysis**

161 The optimum amount of coarse RCA to be added to the mixtures was decided after a preliminary
 162 analysis. Three mixes with 0 %, 50 % and 100 % coarse RCA (labelled C0, C50 and C100 respectively)
 163 were used to mold 10x20-cm cylindrical samples (2 samples in each test). Their compositions are
 164 shown in Table 3. The compressive strength and the modulus of elasticity of the samples were tested
 165 at 7 and 28 days. The results were evaluated with a one-way ANOVA (5 % significance level), which
 166 showed no significant differences between the compressive strength and the modulus of elasticity of
 167 the mixes with 50 % and 100 % of coarse RCA (Table 4). So, an amount of 100 % of coarse RCA was
 168 used in the analysis of the fine RCA mix performance, in order to maximize the sustainability of the
 169 SCC designed.

Mix	C0	C50	C100
Cement	300	300	300
Filler	180	180	180
Water	140	155	165
Siliceous gravel 4/12.5 mm	570	285	0
Coarse RCA 0/12.5 mm	0	265	525
Siliceous sand 0/4 mm	1,150	1,150	1,150
Admixture 1	2.20	2.20	2.20
Admixture 2	4.40	4.40	4.40

170 Table 3. Mix design of the mixes of the preliminary analysis (kg)

Test	Age (days)	Mixes			One-way ANOVA. Factor analyzed: coarse RCA content	
		C0	C50	C100	P-value	Homogeneous groups
Compressive strength (MPa)	7	67.6	57.8	55.7	0.0002	C50 and C100
	28	69.8	61.5	59.3	0.0082	
Modulus of elasticity (GPa)	7	39.7	35.9	34.8	0.0001	
	28	43.4	40.0	39.1	0.0002	

171 Table 4. Hardened properties (average values) and one-way ANOVA of the preliminary analysis

172 **3.2.2. Mixes with fine RCA**

173 Having defined the reference dosage (100 % coarse RCA and 0 % fine RCA), the siliceous sand 0/4 mm
 174 was progressively replaced with fine RCA by volume, in percentages of 25 %, 50 %, 75 %, and finally
 175 100 %. As indicated above, the water content was adjusted to each mix, thereby increasing the water-
 176 to-cement (w/c) ratio and the effective w/c ratio, calculated from the water absorption rate over 10
 177 minutes. The values for these ratios and the mix design can be seen in Table 5. The mixes were labelled
 178 M0, M25, M50, M75, and M100 depending on the percentage of fine RCA. In this table, the dosage of
 179 the mixtures is shown in two different ways. Firstly, in a comparative way, by weight, with respect to
 180 the reference mix M0, so that any changes to the fine RCA and the water content may be easily
 181 observed. Secondly, the dosage of the mixtures adjusted to 1 m³ is shown, so that they may be easily

182 reproduced. Figure 3 shows the overall particle size (corrected by volume) of mixes M0, M50, and
 183 M100, and their Fuller curve.

Mix	Comparative dosage with mixture M0 (kg)					Dosage (kg/m ³)				
	M0	M25	M50	M75	M100	M0	M25	M50	M75	M100
Cement	300	300	300	300	300	300	295	288	282	276
Filler	180	180	180	180	180	180	176	173	169	166
Water	165	187	205	230	250	165	183	198	215	232
Coarse RCA 0/12.5 mm	525	525	525	525	525	525	518	508	497	487
Fine RCA 0/4 mm	0	265	530	795	1,060	0	260	510	748	977
Siliceous sand 0/4 mm	1,150	865	575	290	0	1,150	850	555	272	0
Admixture 1	2.20	2.20	2.20	2.20	2.20	2.20	2.18	2.14	2.10	2.05
Admixture 2	4.40	4.40	4.40	4.40	4.40	4.40	4.32	4.24	4.15	4.06
Approximate volume (l)	1,000	1,018	1,038	1,060	1,083	1,000	1,000	1,000	1,000	1,000
Approximate weight (kg)	2,327	2,307	2,282	2,262	2,237	2,327	2,289	2,238	2,189	2,144
w/c	0.561	0.624	0.688	0.763	0.839	0.561	0.624	0.688	0.763	0.839
Effective w/c	0.459	0.470	0.482	0.506	0.530	0.459	0.470	0.482	0.506	0.530

Table 5. Mix design.

184

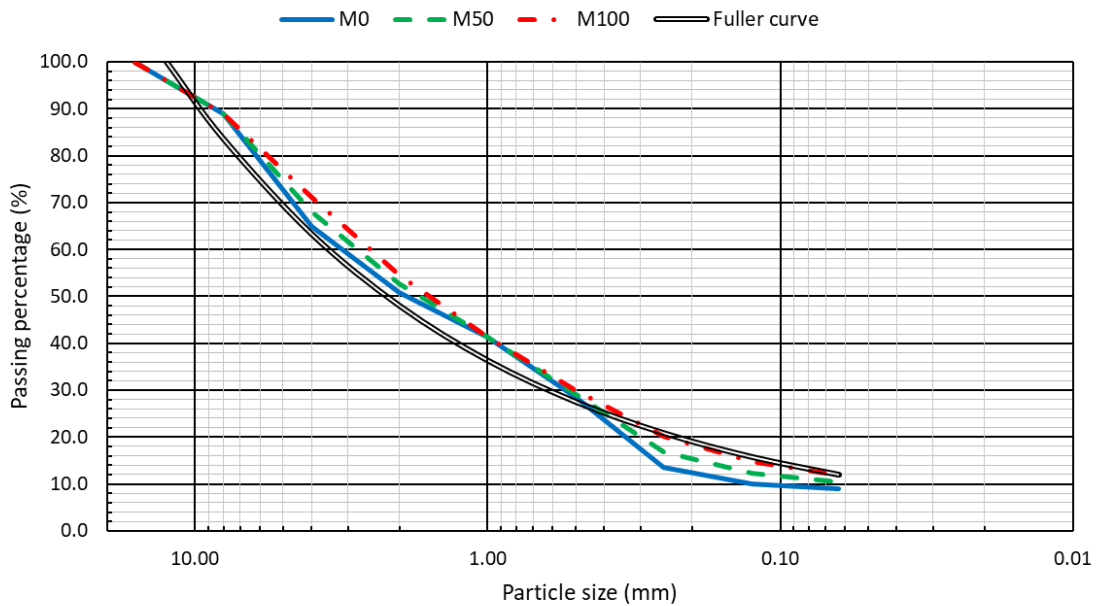


Figure 3. Mix design granulometry.

185

186

187 **3.3. Experimental procedure**

188 A three-stage mixing process was performed for proper hydration of all the components, maximization
 189 of flowability, and to prevent the absorption of additive into the aggregates [40]. First, coarse RCA and
 190 fine fractions (siliceous sand 0/ 4 mm and/or fine RCA) were loaded in the concrete mixer bowl with
 191 half of the mix-water and mixed for 30 s. Then, the cement, filler and the rest of the water were added,
 192 followed by another 30 s of mixing. Finally, the additive dissolved in 0.2 liters of water was added and
 193 mixed for the last 30 s. The aggregates were used under laboratory conditions, at an average

194 temperature and humidity of 20 °C and 45 %, respectively, thus adjusting the experimental procedure
 195 to the most economically advantageous methodology [41].

196 Having completed the mixing process, in-fresh state tests, following the EFNARC recommendations,
 197 were performed [32] and the specimens were molded to carry out the hardened state tests. The tests,
 198 the standards, the age of the test, and the type and the number of test samples at each dosage are
 199 summarized in Table 6. The samples were held in a wet chamber at a humidity of 95 ± 5 % and at
 200 temperature of 20 ± 2 °C until the time of the test. In addition, images from a Scanning Electron
 201 Microscope (SEM) were used to evaluate the quality of the ITZ in one of the worst performing
 202 specimens of mix M75.

Test	Regulations [35]	Test age (days)	Number and type of sample tested per mixture
Slump flow	EN 12350-8		Sample of fresh concrete
V-funnel	EN 12350-9		
2-bar L-box	EN 12350-10		
Sieve segregation	EN 12350-11		
Fresh density	EN 12350-6		
Air content	EN 12350-7		
Compressive strength	EN 12390-3	1, 7, 28, 90	3 cylindrical samples 10x20 cm at each age
Hammer rebound index	EN 12504-2		2 cylindrical samples 10x20 cm at each age
Ultrasonic Pulse Velocity (UPV)	EN 12504-4		2 prismatic samples 10x10x40 cm at each age
Hardened density	EN 12390-7	28	2 cubic samples 10x10x10 cm
Splitting tensile strength	EN 12390-6	7, 28, 90	2 cylindrical samples 15x30 cm at each age
Flexural strength	EN 12390-5		2 prismatic samples 10x10x40 cm at each age
Static modulus of elasticity and Poisson coefficient	EN 12390-13		3 cylindrical samples 10x20 cm at each age
Stress-strain curves	-	90	2 cylindrical samples 10x20 cm
Abrasion resistance	EN 1340 EN 14157		2 cubic samples 10x10x10 cm

203 Table 6. Tests, regulations, and samples used for each mix.

204 The mechanical properties measured by these tests were evaluated both descriptively, which allows
 205 visual detection of differences in the behavior of the mixes, and by statistical analysis through one-way
 206 ANOVA at a significance level of 5 %. This statistical analysis was to study the effect of each factor (age
 207 and fine RCA content) for each mechanical property under study and to establish homogeneous
 208 groups, i.e., factor values for which a certain mechanical property is significantly equal.

209 **3.4. Theoretical calculations**

210 The experimental values of each mechanical property were compared with the theoretical values
 211 obtained from the formulas of the Spanish structural concrete standard EHE-08 [34], an adaptation of
 212 the Eurocode 2 regulation [39], based on the recommendations of the International Federation for
 213 Structural Concrete (CEB-FIP) [42].

214 According to EHE-08 [34], experimental compressive strengths at 28-days can be considered a medium
 215 28-day compressive strength ($f_{c,m}$), with which the characteristic compressive strength ($f_{c,k}$) can be

216 estimated, according to equation (1). Having done so, the medium tensile strength ($f_{ct,m}$) can be
 217 determined, according to equation (2), and the medium flexural strength ($f_{ct,m,fl}$), as a function of the
 218 beam height (h) in mm by applying equation (3). These last two strengths were compared with the
 219 values of splitting tensile strength and flexural strength, experimentally obtained at 28 days.

$$220 \quad f_{c,k} = f_{c,m} - 8 \quad (1)$$

$$221 \quad \begin{cases} f_{ct,m} = 0.30 \cdot f_{c,k}^{2/3} & \text{if } f_{c,k} \leq 50 \text{ MPa} \\ f_{ct,m} = 0.58 \cdot f_{c,k}^{1/2} & \text{if } f_{c,k} > 50 \text{ MPa} \end{cases} \quad (2)$$

$$222 \quad f_{ct,m,fl} = \max \left\{ \left(1.6 - \frac{h}{1,000} \right) \cdot f_{ct,m}; f_{ct,m} \right\} \quad (3)$$

223 EHE-08 [34] specifies the formula for estimating the static concrete elasticity modulus at any age,
 224 equation (4). The expression contains the following factors: curing time in days (t); the 28-day secant
 225 modulus of elasticity ($E_{c,m}$) calculated with equation (5); the medium compressive concrete strength at
 226 t days ($f_{c,m}(t)$), obtained with equation (6); and, the secant modulus of elasticity at t days ($E_{c,m}(t)$). The
 227 units of strength and the modulus of elasticity in all the expressions can only be introduced in
 228 Megapascals (MPa).

$$229 \quad E_{c,m}(t) = \left(\frac{f_{c,m}(t)}{f_{c,m}} \right)^{0.3} \cdot E_{c,m} \quad (4)$$

$$230 \quad E_{c,m} = 8,500 \cdot \sqrt[3]{f_{c,m}} \quad (5)$$

$$231 \quad f_{c,m}(t) = \exp \left\{ 0.2 \cdot \left[1 - \left(\frac{28}{t} \right)^{1/2} \right] \right\} \cdot f_{c,m} \quad (6)$$

232 The structural concrete design guidelines of the American Concrete Institute (ACI) [38] contain
 233 formulas, equations (7) and (8), for calculating the tensile strength of concrete and its modulus of
 234 elasticity from its compressive strength, respectively. The variables of the equation refer to
 235 compressive strength, (f_c), tensile strength, (f_t), and the modulus of elasticity, (E). These expressions
 236 are easier to apply than those indicated above, and their validity is also analyzed in this study.

$$237 \quad f_t = 0.56 \cdot f_c^{0.5} \quad (7)$$

$$238 \quad E = 4,700 \cdot \sqrt{f_c} \quad (8)$$

239 Simple regression equations are provided, to complement this analysis, which were developed for the
 240 mechanical properties (splitting tensile strength, flexural strength, and modulus of elasticity)
 241 measured in this study. These formulas can be used as a basis for more general models taken from the
 242 literature, for accurate estimation of the properties of SCC made with RCA.

243 On the other hand, the value of the dynamic modulus of elasticity (E_d) at different ages of curing can
244 be calculated from the test results with equation (9) [33], using the density of the concrete (ρ), the
245 UPV (V_t), and the Poisson coefficient (ν). All the above-mentioned properties were precisely
246 established with the tests performed.

$$247 \quad E_d = \rho \cdot V_t^2 \cdot \frac{(1+\nu) \cdot (1-2 \cdot \nu)}{1-\nu} \quad (9)$$

248 **4. Results and discussion**

249 The experimental results of the in-fresh and the hardened states, as well as the theoretical estimation
250 of the mechanical properties from the concrete design standards are presented in this section.

251 **4.1. Fresh properties**

252 It is clear from the bibliography that the addition of RCA clearly reduces the flowability of the SCC, due
253 to its higher water absorption, resulting in a lower effective w/c ratio for any given w/c ratio without
254 RCA [20; 33; 43]. In addition, the crushing process of the RCA produces irregular shapes, which means
255 that the aggregate particles will not flow easily in the paste [44; 45]. Although the effective w/c ratio
256 decreases with the coarse RCA, its irregular shaped particles have the most notable effects [33; 46].
257 The predominant effect of the fine RCA results from its high level of water absorption that decreases
258 the effective w/c ratio [43]. Regarding the maximum diameter obtained in the slump-flow test, the
259 decrease in initial flowability is as much as 36 % with 100 % coarse RCA and up to 19 % with 100 % fine
260 RCA [43-45].

261 The adjustment of the water absorbed by the RCA solves the water absorption problem, preventing
262 the effective w/c ratio from decreasing [19; 37]. Another possibility is to increase the proportion of
263 the finest aggregate fraction (<0.125 mm), thereby increasing the volume of paste. Balanced
264 proportions of fine and coarse aggregates are therefore fundamental for good performance of SCC
265 [21].

266 In the concretes under study, the water content was adjusted by increasing the percentage of fine RCA
267 aggregate, thereby increasing the effective w/c ratio. In addition, that increase of fine RCA aggregate
268 also led to an increase in the fine fraction (<0.125 mm) within the overall granulometry of the mixtures.
269 Both aspects compensated the negative effects of RCA and even improved the slump flow and the
270 passing ability of the SCC. Some of the in-fresh state tests are shown in Figure 4 and their results,
271 presented in Table 7, are consistent with the above-mentioned aspects.

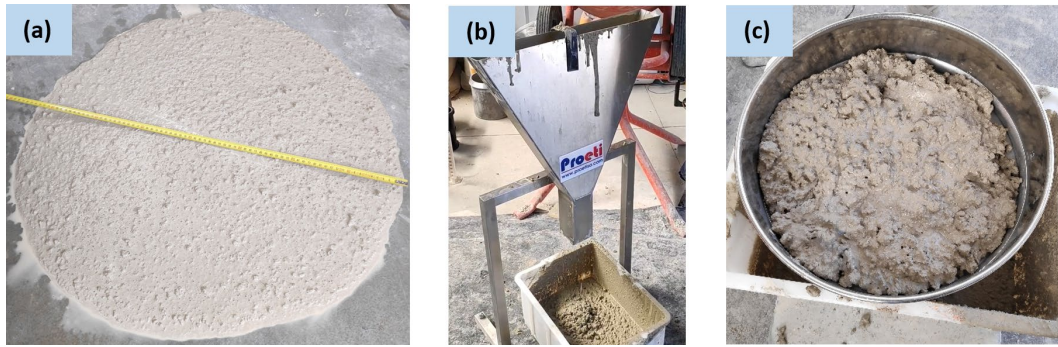


Figure 4. In-fresh state tests for M50 mix. (a) slump-flow; (b) V-funnel; (c) sieve segregation

Test/Mix	M0	M25	M50	M75	M100
Viscosity t_{500} slump flow test (s)	3.40	3.60	4.00	4.20	4.80
Slump flow (mm)	680	695	730	740	755
Viscosity V-funnel test (s)	6.40	8.40	10.20	12.60	15.20
Passing ability L-box test H_2/H_1	0.86	0.88	0.92	0.93	0.94
Sieve segregation (%)	1.70	1.52	1.67	1.53	1.36
Air content (%)	4.80	3.75	4.35	4.00	4.15
Fresh density (Mg/m^3)	2.40	2.31	2.25	2.16	2.12

Table 7. In-fresh state test results

As reported in similar studies [43], the lower density of the RCA, compared to the NA, and the increase in water content decreased the fresh density of the SCC [46; 47]. The air content, very similar in all mixtures, mainly depended on the admixtures and the chemical reactions they produced, with no clear influence of fine RCA.

Based on the results of the in-fresh state tests and the EFNARC recommendations [32], the developed SCCs presented:

- A slump-flow class SF2 (maximum diameter between 660 and 760 mm).
- A viscosity class, according to the slump-flow test, VS2 (time to reach a diameter of 500 mm greater than 2s) and, according to the V-funnel test, VF2 (time to empty the V-funnel greater than 8s), except for the M0 mixture which was class VF1.
- A passing-ability class PA1, according to the 2-bar L-box test (blocking ratio greater than 0.80).
- A segregation-resistance class SR2 (sieve segregation less than 15 %).

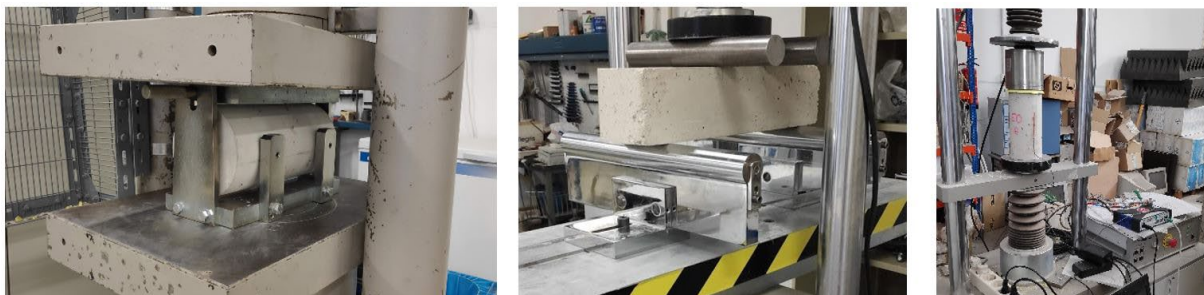
The maximum diameter in the slump-flow test increased by 11 % (from 680 mm for M0 to 752 mm for M100), following the addition of 100 % fine RCA, which in turn increased the effective w/c ratio by 15 % (from 0.46 to 0.53). In this case, the passing ability was also increased by 9 % (from 0.86 to 0.94). The fines content of the mix M25 influenced the flowability of the SCC. A fine RCA content of 25 % and an effective w/c ratio of 0.47, slightly higher than 0.46 (corresponding to mix M0), led to a higher slump flow and passing ability. However, it was not possible to compensate all the negative effects of RCA by increasing the proportion of water and fines, as viscosity was negatively affected, resulting in higher slump-flow viscosity and emptying times (V-funnel test). This performance can be explained by two

295 aspects: the irregular shapes of the coarser fine RCA particles that move more slowly within the cement
 296 paste than the rounded siliceous sand particles; and the higher proportion of cement paste, resulting
 297 from the increased volumes of fines, following the addition of RCA, leaving the SCC with a more viscous
 298 consistency.

299 Resistance to segregation was not negatively affected by the addition of fine RCA and was even
 300 improved by the increase of the fine RCA content. In fact, the sieve segregation of the mixture M100
 301 (1.36 %) was 25 % lower than that of the mixture M0 (1.70 %). Even though fine RCA had a higher
 302 content of particles smaller than NA (≤ 0.125 mm), the use of fine RCA produced higher long-term water
 303 absorption levels that reduced segregation.

304 **4.2. Hardened state behavior**

305 The analysis of the mechanical properties aims to evaluate the effect of fine RCA on the development
 306 of strength at different curing ages. Some of these tests, such as for splitting tensile strength, flexural
 307 strength, and modulus of elasticity, are shown in Figure 5.



308
 309 Figure 5. Mechanical tests: splitting tensile strength (left); flexural strength (middle); modulus of
 310 elasticity (right)

311 **4.2.1. Density**

312 The lower density of RCA compared to NA reduced the hardened density of the SCC, as the RCA content
 313 increased (Table 8), in line with the existing bibliography [33; 37; 48]. The decrease of the hardened
 314 density compared to the fresh density showed no clear trends, although it was higher in the mixtures
 315 with a higher NA content (mixture M0 showed a decrease of 4.2 %, while this decrease for mixture
 316 M50 was only 0.4 %), which may be due to the lower water evaporation, because of the higher water
 317 absorption of fine RCA [33].

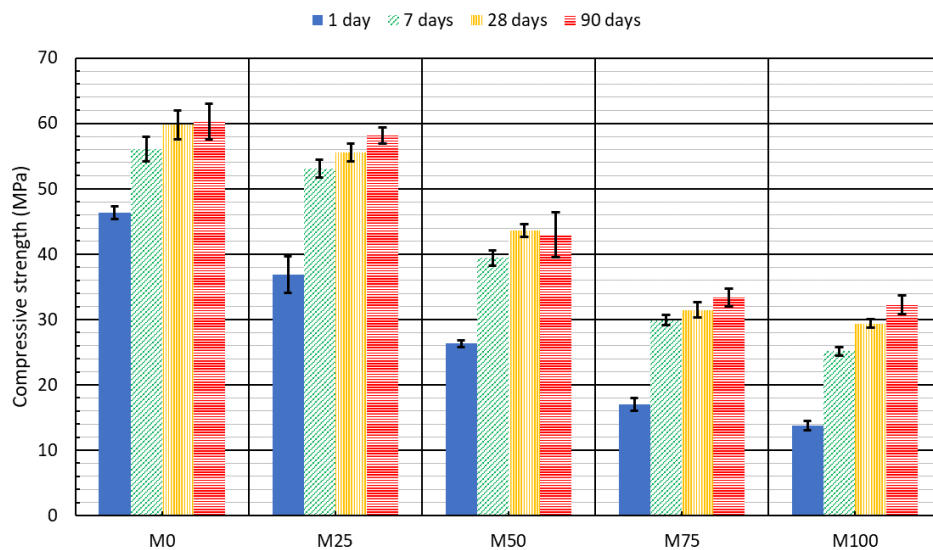
Test/Mix	M0	M25	M50	M75	M100
Hardened density (Mg/m ³)	2.30	2.29	2.24	2.13	2.10
Decrease with respect to its fresh density (%)	4.2	0.9	0.4	1.4	1.0
Decrease with respect to the M0 density (%)	0	0.4	2.6	7.4	8.7

318 Table 8. Hardened density of the mixes

319 **4.2.2. Compressive strength, UPV, and hammer rebound index**

320 The addition of coarse RCA is known to reduce the compressive strength of concrete [49], although
321 reductions of just 5 MPa for 100 % coarse RCA content were obtained in some studies [45; 50]. The
322 reduction was higher when fine RCA was added [36], and in some studies the decrease caused by 100 %
323 fine RCA in SCC reached 26 % compared to the reference concrete (0 % coarse and fine RCA) [20; 51].
324 Nevertheless, if the effective w/c ratio is reduced, the loss of strength can be compensated, especially
325 when only coarse RCA is used [33; 46]. In the present study, as expected, the compressive strengths of
326 the concretes under study decreased as their fine RCA content increased and with it, the w/c ratio
327 (Table 5), as shown in Figure 6. At 28 days, the decrease in strength, with regard to the reference
328 mixture M0 (60 MPa), was 7 % for mixture M25 (56 MPa), 27 % for mixture M50 (44 MPa), and 47 %
329 and 51 % for mixtures M75 and M100, respectively (strengths of 31 and 30 MPa). Regarding the overall
330 trend, mixture M25 showed a much lower than expected strength decrease, possibly due to its very
331 similar effective w/c ratio to mix M0.

332 The compressive strength results showed less dispersion with higher additions of fine RCA content,
333 although that dispersion increased at advanced ages. The strengths of the mixtures with high RCA
334 contents were more closely limited at early ages.

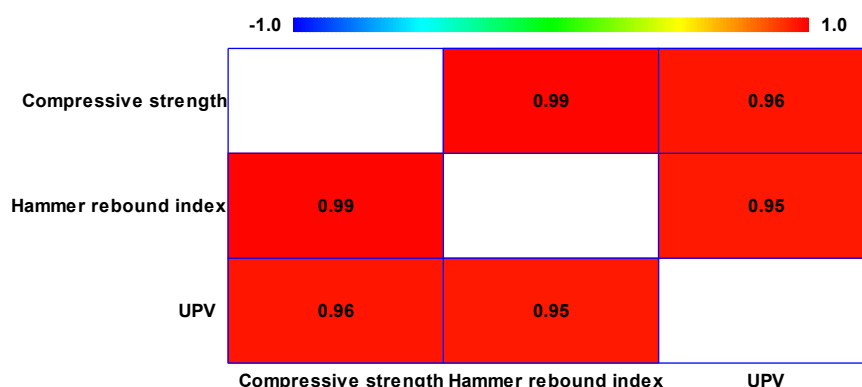


335
336

Figure 6. Compressive strength of the SSC mixtures

337 The compressive strength developed at 1 and 7 days, with regard to the strength at 28 days, were in
 338 percentage terms 78 % and 94 % for the reference mix, M0; 60 % and 90 % for M50; and 47 % and
 339 86 % for M100. Strength development, in percentage terms, was slower as the fine RCA content
 340 increased.

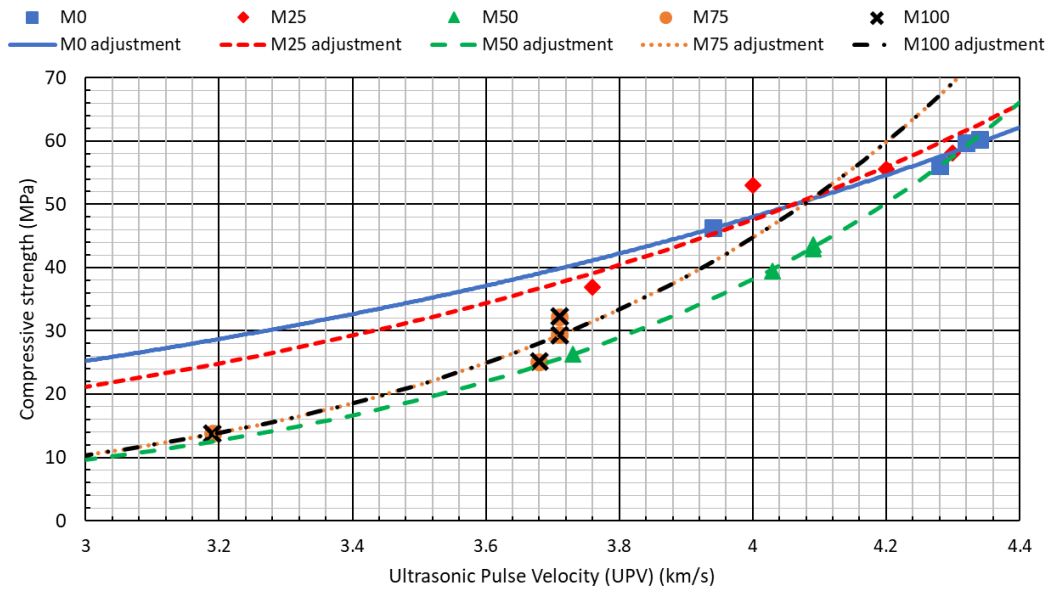
341 The UPV and the hammer rebound tests, two conventional methods for estimating the compressive
 342 strength of non-recycled concrete, were measured at all ages. Pearson's symmetrical correlation
 343 matrix between these three properties for all mixtures and ages simultaneously is shown in Figure 7.
 344 A clear linear relationship between these variables can be observed, as in other similar studies [28;
 345 52], although an individual analysis carried out in each mix showed that the exponential model had
 346 the best overall fit. Table 9 shows the least square exponential adjustment of compressive strength
 347 (variable "y") as a function of the UPV (variable "x") and the hammer rebound index (variable "z"). The
 348 adjustment had a coefficient R² higher than 0.90 in 80 % of the cases. Mixture M100 had the
 349 coefficients R² closest to 1.00. The validity of these indirect measures was not influenced by the
 350 addition of RCA. Figure 8 and Figure 9 show this adjustment for each mixture and it may be noted that
 351 the increase in RCA content increased the curvature of the models.



352
 353 Figure 7. Pearson's symmetrical correlation matrix for compressive strength, hammer rebound index
 354 and UPV

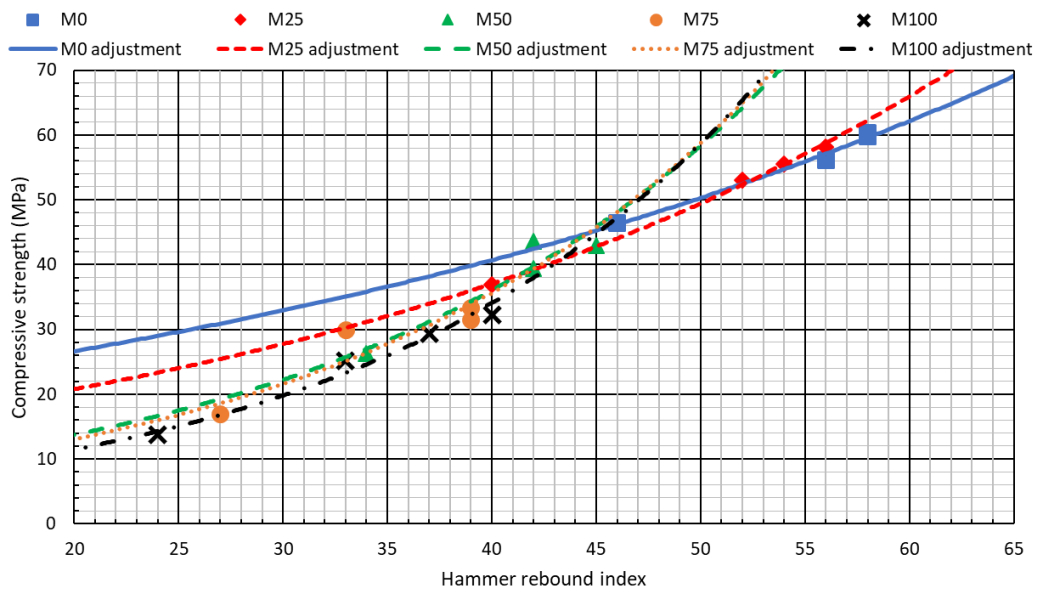
Test/Mix		M0	M25	M50	M75	M100
UPV (km/s)	1 day	3.94	3.76	3.73	3.27	3.19
	7days	4.28	4.00	4.03	3.63	3.68
	28 days	4.32	4.20	4.09	3.80	3.71
	90 days	4.34	4.30	4.09	3.79	3.71
Exponential adjustment: compressive strength-UPV		$y=3.666 \cdot \exp(0.643x)$	$y=1.854 \cdot \exp(0.811x)$	$y=0.155 \cdot \exp(1.376x)$	$y=0.312 \cdot \exp(1.232x)$	$y=0.130 \cdot \exp(1.461x)$
Coefficient R ² UPV		0.96	0.87	0.99	0.95	0.98
Hammer rebound index	1 day	46	40	34	27	24
	7days	56	52	42	33	33
	28 days	58	54	42	39	37
	90 days	58	56	45	39	40
Exponential adjustment: compressive strength- hammer rebound index		$y=17.443 \cdot \exp(0.021z)$	$y=11.669 \cdot \exp(0.029z)$	$y=5.236 \cdot \exp(0.048z)$	$y=4.804 \cdot \exp(0.050z)$	$y=3.871 \cdot \exp(0.054z)$
Coefficient R ² hammer rebound index		0.98	0.99	0.92	0.85	0.98

355 Table 9. Exponential adjustment between UPV and hammer rebound index and compressive strength



356
357

Figure 8. Adjustment of the compressive strength as a function of the UPV

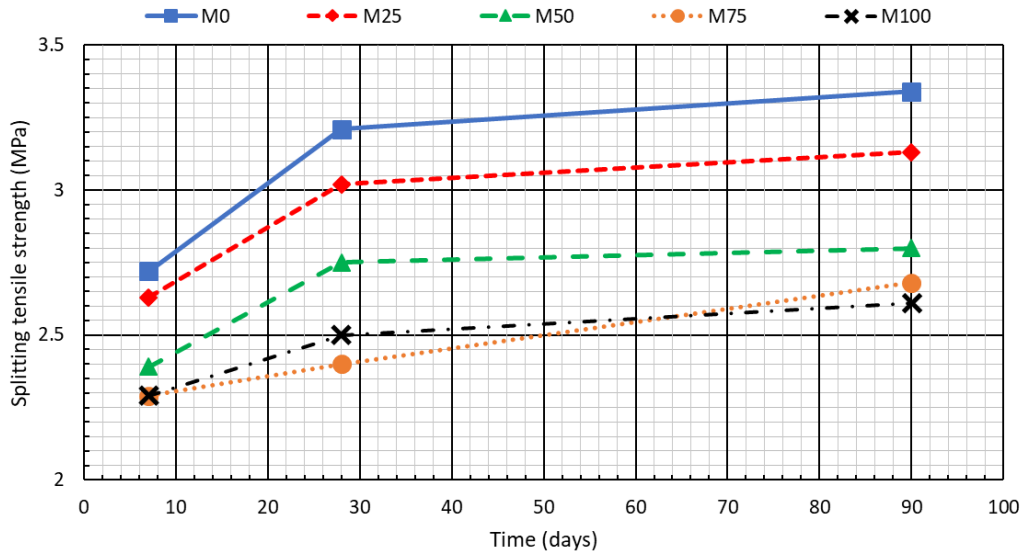


358
359

Figure 9. Adjustment of the compressive strength as a function of the hammer rebound index

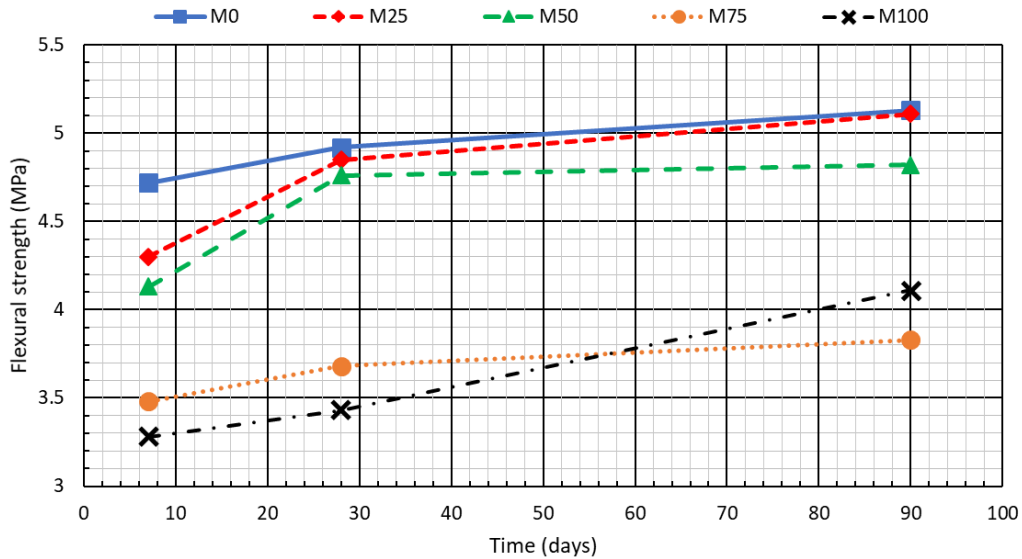
360 **4.2.3. Splitting tensile strength and flexural strength**

361 The results, obtained at 7, 28, and 90 days, showed that the addition of fine RCA decreased both the
 362 splitting tensile strength (Figure 10) and the flexural strength (Figure 11), a widely reported behavior
 363 in the literature [33; 37; 51]. The harmful effect of fine RCA can be compensated and if the dosage is
 364 correctly modified, it is possible to obtain a splitting tensile strength equal to that of the reference
 365 concrete [27]: reducing the water content, increasing the cement content, or using alternative binders
 366 such as fly ash or silica fume [53; 54].



367
368

Figure 10. Splitting tensile strength



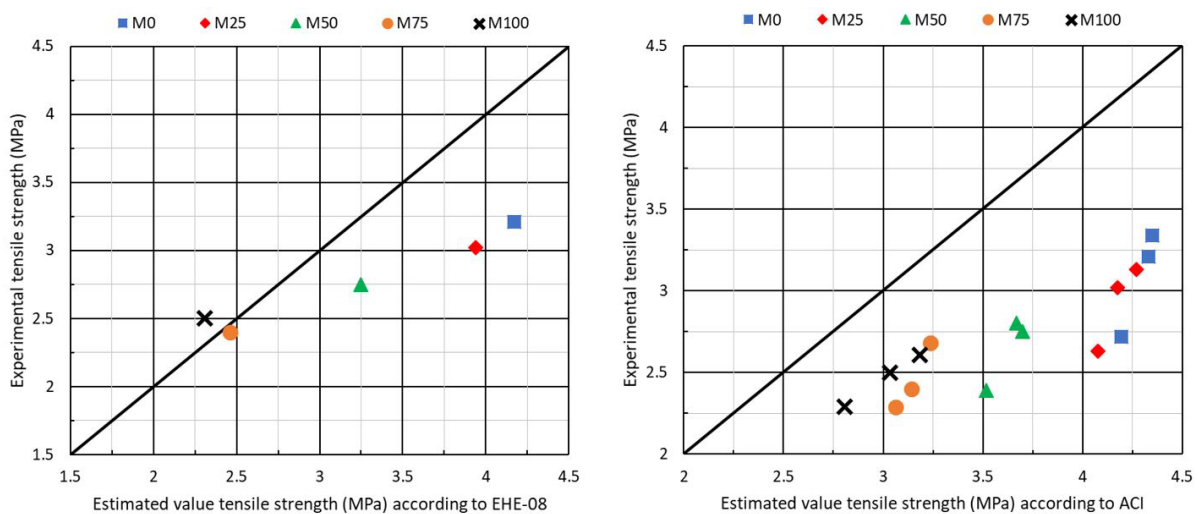
369
370

Figure 11. Flexural strength

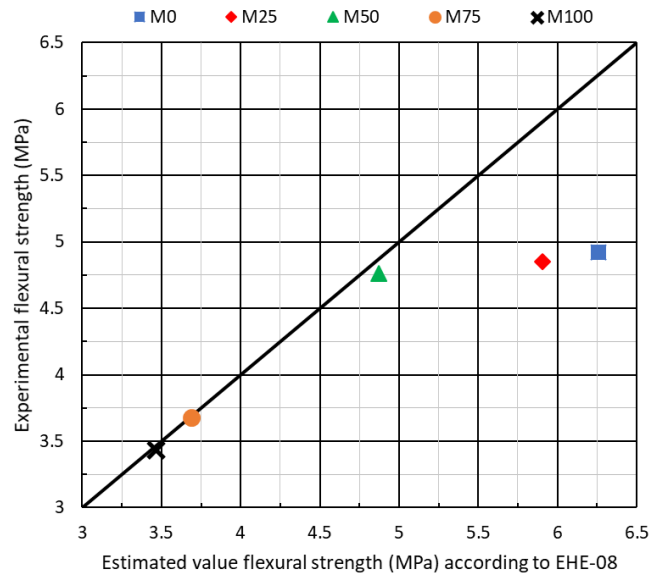
371 In this study, the decrease was mainly observed for the flexural strength, with different behavior in
 372 two groups (fine RCA up to 50 % and above 50 %). Compared to M0, the decrease of the flexural
 373 strength at 28 days of the mixture M100 was 30 % (3.4 versus 4.9 MPa) and was only 22 % for the
 374 splitting tensile strength (2.5 versus 3.2 MPa). However, there were some exceptions, such as the
 375 higher flexural strength of mix M100 compared to M75 at 90 days, due to the low adhesion between
 376 the cement paste and the coarse aggregate, in the mixes with high fine RCA content. It was observed
 377 that high additions of fine RCA also favored a more uniform strength over time, and a less predictable
 378 behavior.

379 Some studies have shown that the theoretical tensile strength value, calculated according to the EC2
 380 [39], was lower than the experimental value in SCC made with coarse RCA, whilst the experimental

381 value was overestimated in SCCs with high fine RCA content [37]. The theoretical tensile strength
 382 values as per EHE-08 [34], shown in Figure 12 and calculated with equation (2), were higher than the
 383 experimentally obtained results for all the mixtures in this study, although the adjustment was
 384 improved by increasing the fine RCA content (the experimental tensile strength of M100 was higher
 385 than the theoretical value). In relation to the values estimated with equation (7) from the ACI [38], it
 386 can be observed that the theoretically calculated values also overestimated the results. The SCCs with
 387 the highest fine RCA content were those that showed the least difference between both values: in M0,
 388 the theoretical value at 28 days (4.3 MPa) was 34 % higher than the experimental value (3.2 MPa),
 389 while this overestimation in the mixture M100 was only 20 % (3.0 versus 2.5 MPa). As the increase in
 390 compressive strength after 7 days was higher than the increase in splitting tensile strength, the
 391 adjustment was better for advanced ages. Similarly, the design values of flexural strength (Figure 13)
 392 also overestimated the experimental values, once again with a better fit as fine RCA was added. From
 393 all the above, it can be deduced that both the splitting tensile strength and the flexural strength were,
 394 in general, lower than expected, especially in the case of concretes with few recycled fines. The use of
 395 the equations from the standards applied to the test mixtures would imply strength overestimations
 396 of around 25 %, especially with fine RCA contents up to 50 %.



397
 398 Figure 12. Relationship between the experimental tensile strength and the estimated value as per
 399 EHE-08 (left) and ACI (right)



400 Figure 13. Relationship between the experimental flexural strength and the estimated value as per
 401 EHE-08
 402

403 The standard formulas [34; 38] relate both tensile strength and flexural strength to compressive
 404 strength by means of a square or cubic root. Nevertheless, the best-fit model (coefficient R^2 of 0.86)
 405 of the splitting tensile strength (STS , in MPa) as a function of compressive strength (CS , in MPa), shown
 406 in equation (10), established a polynomial relationship between both variables. In contrast, the flexural
 407 strength (FS , in MPa), equation (11), with a coefficient R^2 of 0.88, has an inverse relationship with the
 408 compressive strength.

409
$$STS = 8.46 - 0.79 \cdot CS + 0.04 \cdot CS^2 \quad (10)$$

410
$$FS = \left(2.55 - \frac{19.26}{CS} \right)^2 \quad (11)$$

411 **4.2.4. Static modulus of elasticity and Poisson coefficient**

412 The presence of adhered mortar and the ITZs, which were weak and not very dense, meant that the
 413 SCC with RCA was, in general, more deformable than the SCC with NA [25; 33], observations supported
 414 by the results from this study that are shown in Figure 14. A higher fine RCA content led to a lower
 415 modulus of elasticity at all ages: at 28 days, M100 presented a modulus of elasticity of 18.8 GPa, 54 %
 416 lower than the mix M0 (40.6 GPa). The addition of 100 % fine RCA to an SCC with 100 % coarse RCA,
 417 as performed in this study, led to a greater decrease in the modulus of elasticity than when this amount
 418 of fine RCA is added to an SCC with no coarse RCA, which is around 24 % [37; 51].

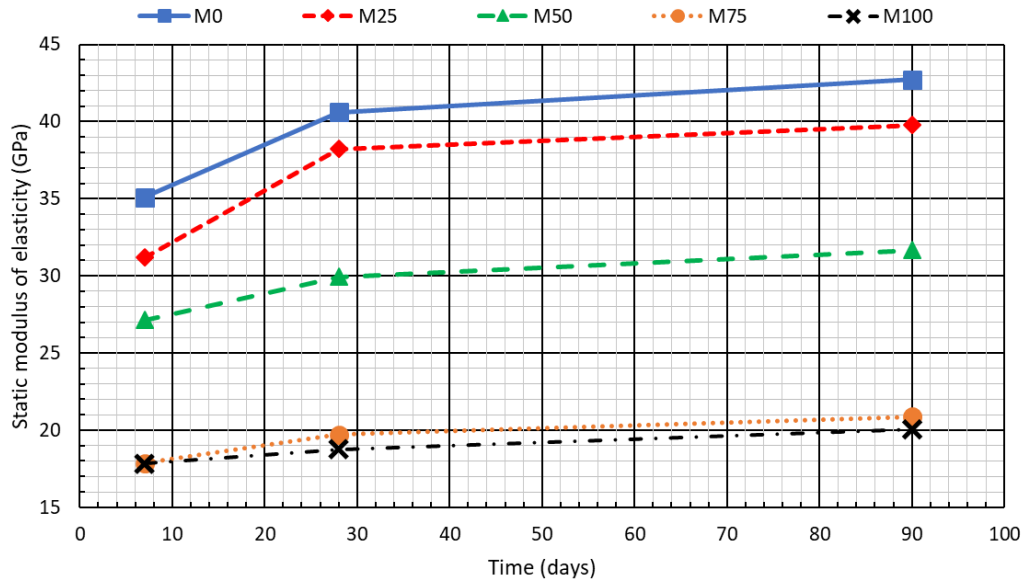
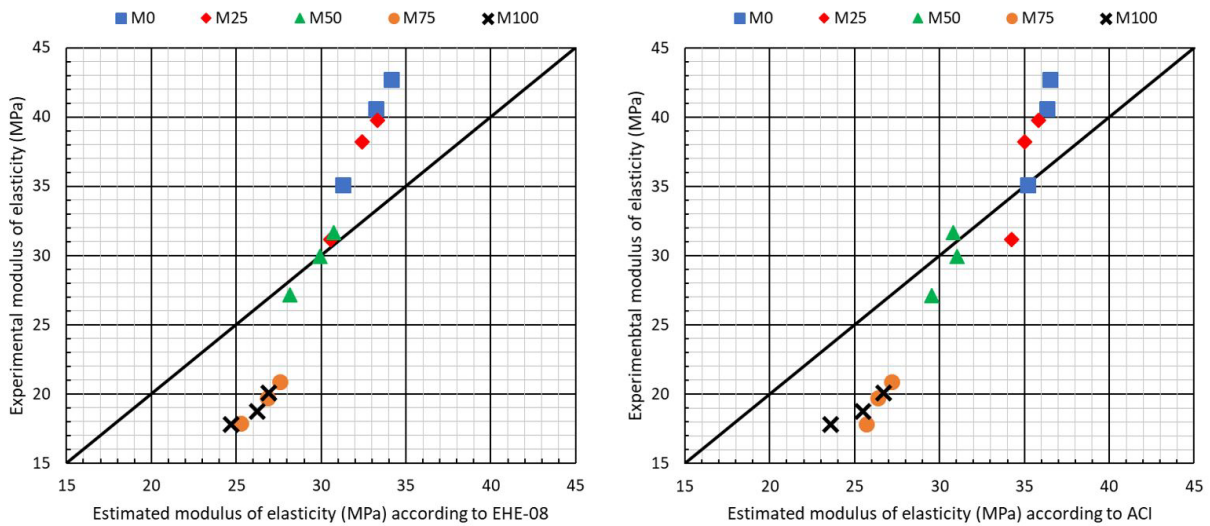


Figure 14. Static modulus of elasticity

419
420

421 The trends for the modulus of elasticity over the curing, once again showed a different behavior
422 between the mixtures with low/medium percentages and those with high percentages of fine RCA: the
423 mixtures with low percentages of fine RCA (M0 and M25) showed a very marked increase in the
424 modulus of elasticity up to 28 days, while the increase in concretes with higher contents (M75 and
425 M100) was practically uniform over time.

426 The adjustment of the theoretical values, obtained with equation (4), to the experimental values was
427 quite poor (Figure 15). In mixtures with low percentages of fine RCA (M0 and M25), the design values
428 were lower than the experimental values (at 28 days, the design value of mixture M25 was 32.4 GPa,
429 15 % lower than the experimental value, 38.2 GPa). The theoretical expressions overestimated the
430 modulus of elasticity in the mixtures with high contents of fine RCA (M75 and M100), by approximately
431 40 % at all ages of curing. Mixture M50 was in an intermediate situation: its theoretical value at 7 days
432 (28.2 GPa) was higher than the experimental value (29.9 GPa), with the opposite situation at 90 days
433 (theoretical value of 30.7 GPa and experimental value of 31.7 GPa). The same situation was observed
434 for the ACI [38] formula, once again showing that mixture M50 had the best fit. These results are in
435 line with the conclusions of other studies, which also showed that the theoretical expressions
436 underestimated the modulus of elasticity in SCCs with low percentages of RCA and overestimated it in
437 mixtures with high percentages of RCA [37; 55].

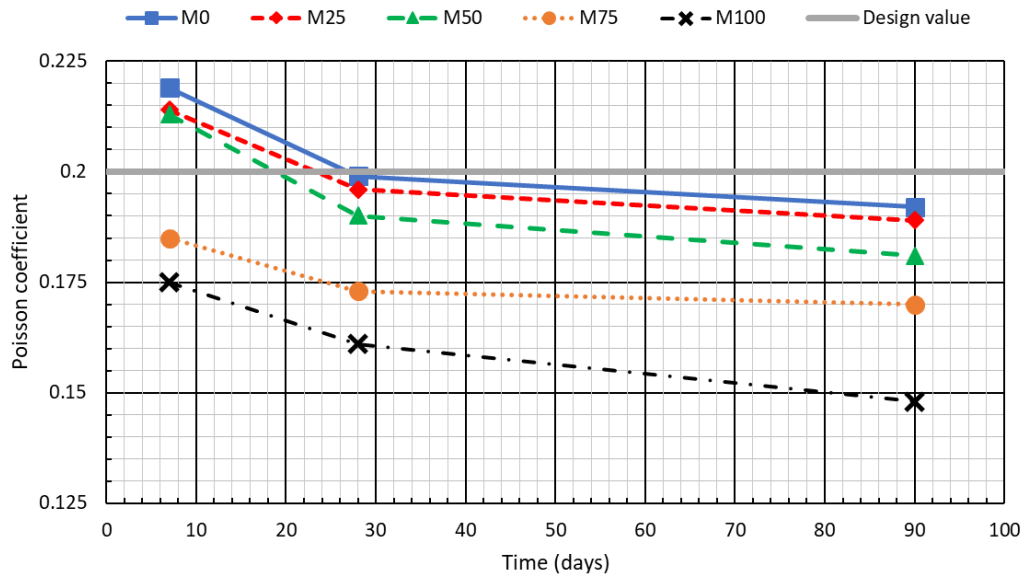


438
 439 Figure 15. Relationship between compressive strength and modulus of elasticity according to EHE-08
 440 (left) and ACI (right)

441 Equation (12) shows that there is an exponential relationship between the modulus of elasticity (ME ,
 442 in GPa) and the logarithm of compressive strength (CS , in MPa), similar to that shown by EHE-08 [34]
 443 in equation (6). Its coefficient R^2 is 0.96.

444
$$ME = \exp(-0.62 + 1.05 \cdot \ln(CS)) \quad (12)$$

445 Increasing percentages of fine RCA increased both the deformability of the concrete in the load
 446 direction and the volume variation under load, as shown by the lower Poisson coefficient (Figure 16)
 447 of the concrete with additions of fine RCA: after 28 days, the difference of the Poisson coefficient
 448 between mixtures M0 (0.20) and M100 (0.16) was 19 %. This trend was similar to the one obtained in
 449 vibrated concretes with only coarse RCA [56; 57], although a constant w/c ratio appeared to prevent
 450 the Poisson coefficient from decreasing [58]. The temporal evolution of this coefficient was similar in
 451 all the mixtures: a marked decrease in the first days, less noticeable as time goes by, although M100
 452 showed a much more remarkable decrease after 28 days than the rest of the mixtures. The
 453 conventional value of the Poisson coefficient for concrete (0.2) was higher than the experimental
 454 values, except for concretes with less than 50 % fine RCA at 7 days, that had slightly higher
 455 experimental values.

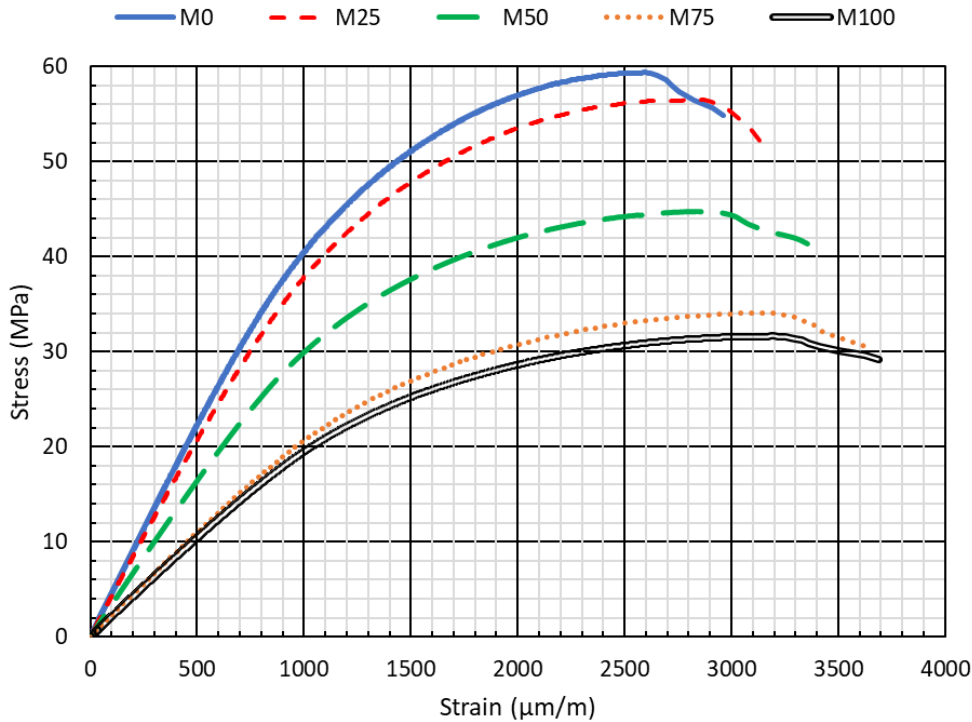


456
457

Figure 16. Poisson coefficient

458 **4.2.5. Stress-strain curves**

459 The stress-strain curves that are used to evaluate the plastic behavior of concrete usually show an
 460 elastic behavior at low load levels and reduced fracture strain values (theoretical value of 3,500 $\mu\text{m}/\text{m}$)
 461 [34; 38; 39]. Higher fines contents will usually result in higher strain values after the ultimate strength
 462 value of the concrete is reached [59]. When this aspect was addressed in recycled concrete, it was
 463 concluded that coarse RCA reduced fracture strain [60]. No reference to this behavior was found for
 464 SCCs made with coarse and fine RCA, such as those reported in this article. Cylindrical specimens of 10
 465 and 20 cm in diameter and height, respectively, were subjected to compressive strength tests until
 466 failure at 90 days, yielding the curves shown in Figure 17. The stress and strain values were recorded
 467 at a frequency of 15 Hz.



468
469

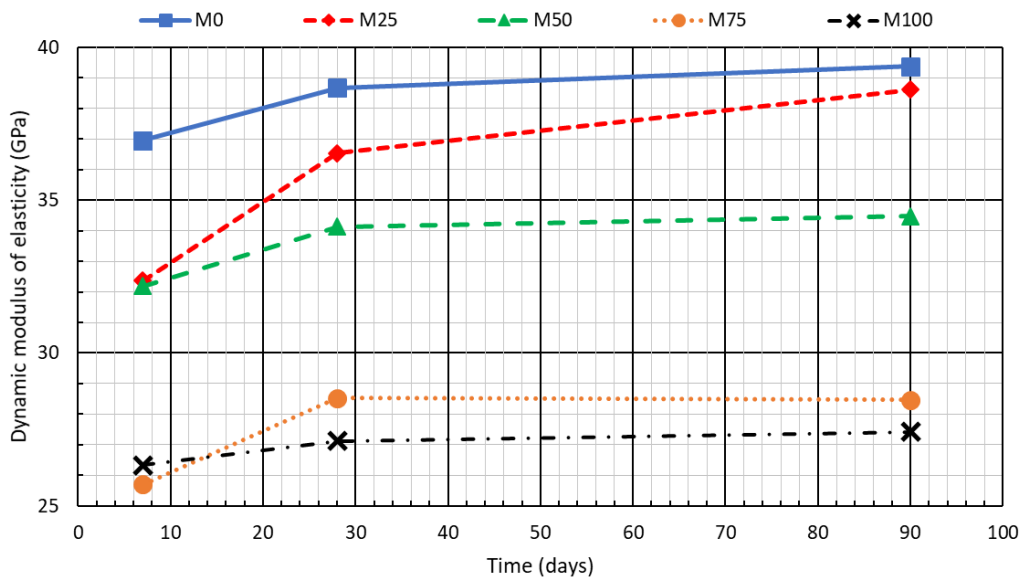
Figure 17. Stress-strain curves of the mixtures

470 The stress-strain curves reflected the decrease, both in compressive strength (ultimate strength) and
471 in the modulus of elasticity, as the fine RCA content increased, as previously discussed (section 4.2.2).
472 Other relevant aspects of the structural design with this type of concrete are:

- 473 • The proportional limit (the point where linear elastic strain ends) was produced for a
474 deformation of 720 $\mu\text{m/m}$ for M0 and 580 $\mu\text{m/m}$ for M100, increasing the plastic deformation
475 with the fine RCA content.
- 476 • An increase in the fine RCA content led to a higher fracture strain: mixtures M0 and M25
477 showed strain values that were 18.9 % lower than mixtures M75 and M100 (3,000 $\mu\text{m/m}$
478 versus 3,700 $\mu\text{m/m}$). The strain values of mixture M50 (3,300 $\mu\text{m/m}$) were the closest to the
479 theoretical value. Thus, the mixtures with higher fine RCA contents presented higher safety
480 design coefficients, as they exceeded the theoretical values calculated with the formulas from
481 the standards. This behavior was contrary to the one observed when only coarse RCA was
482 added [60].
- 483 • The strain values corresponding to the ultimate strength increased with higher contents of fine
484 RCA in the mixtures (2,650 $\mu\text{m/m}$ for mixture M0 and 3,250 $\mu\text{m/m}$ for mixture M100). The
485 ratios between the fracture strain and peak strain for mixtures M0 and M100 were 1.16 and
486 1.13, respectively, and the remaining strain after breakage increased in SCCs with low fine RCA
487 contents. The reference specimen, mixture M0, showed the highest safety factor after failure.

488 **4.2.6. Dynamic modulus of elasticity through the UPV**

489 The dynamic modulus of elasticity decreased with the addition of fine RCA. According to other studies,
490 in mixtures with 50 % coarse RCA, the decrease was approximately 4 %, reaching 9 % for 100 %
491 replacements [33; 61]. No other study has been found in which this property is evaluated in SCCs with
492 fine RCA. The results of this study (Figure 18) showed the same overall trend as the static modulus of
493 elasticity (Figure 14), both in terms of fine RCA content and its temporal evolution. The results for all
494 properties based on the calculation of this modulus of elasticity, according to equation (9), were
495 consistent with each other.



496 Figure 18. Dynamic modulus of elasticity through the UPV

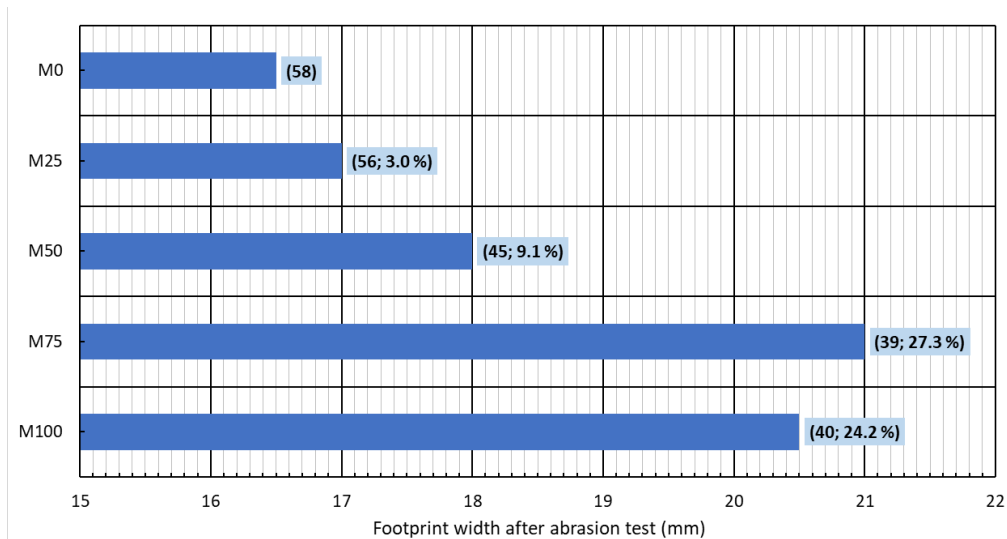
497 Two groups of concretes may be distinguished: high and low/medium fine RCA content. Mixtures with
498 fine RCA content of less than 50 % had a lower dynamic modulus of elasticity through the UPV than
499 the static modulus of elasticity (e.g. the values of the static and dynamic modulus of elasticity of M25
500 at 28 days were 38.2 and 36.5 GPa respectively). Meanwhile mixtures M75 and M100 showed higher
501 stiffness under dynamic loading: the dynamic modulus of elasticity through the UPV of mixture M100,
502 at 28 days, was 44.1 % higher than the static modulus of elasticity (27.1 GPa versus 20.1 GPa).
503

504 **4.2.7. Abrasion resistance**

505 Resistance to abrasion was evaluated by the footprint caused by an abrasive disc on the surface of the
506 material on cubic samples of 10x10x10 cm at 90 days (Figure 19), which measures the hardness of the
507 surface cement paste [62]. According to other studies, the addition of fine RCA increased the size of
508 the footprint [63]. Nevertheless, the use of RCA from a concrete with a strength of over 70 MPa can
509 improve the surface resistance of the concrete [64].



510
 511 Figure 19. Abrasion test. Left: footprint on the M50 mix. Right: sample set up in the testing machine
 512 In this research, the increase in fine RCA generated a cement paste with a lower surface hardness,
 513 which increased the footprint size, as shown in Figure 20. These results were in line with the results of
 514 the 90-day rebound index: a higher rebound index was produced in those mixtures with a smaller
 515 footprint width (mix M75 had a lower rebound index, 39, and a footprint size of 21 mm that was 27.3 %
 516 larger than the M0 footprint). Once again, there were two different groups of concretes, according to
 517 the results of this test: high and low/medium fine RCA content.



518
 519 Figure 20. Resistance to abrasion test results. The hammer rebound index and the increase in
 520 footprint size, in relation to mixture M0, are shown between brackets.

521 **4.2.8. Statistical analysis of mechanical properties**

522 The descriptive analysis was completed with a statistical analysis based on one-way ANOVA (Table 10).
 523 It showed that both age and fine RCA content significantly influenced the behavior of the mixes in all
 524 tests (p-value lower than the significance level considered, 0.05). The homogeneous groups revealed
 525 that, in general, mixes M0 and M25, as well as M75 and M100, have no significant difference in their
 526 mechanical properties regardless the age. In contrast, the mechanical properties of mixes with low fine
 527 RCA contents (M0 and M25) hardly showed significant variations between 28 and 90 days, while the
 528 mechanical properties of mixes M75 and M100, at 7, 28 and 90 days, can be considered statistically
 529 equal in several tests. Mix M50 showed an intermediate behavior.

Test	Factor	Condition	P-value	Homogeneous groups
Compressive strength	Fine RCA percentage	Age of 1 day	0.0001	M75 and M100
		Age of 7 days	0.0001	M0 and M25; M75 and M100
		Age of 28 days	0.0002	M0 and M25; M75 and M100
		Age of 90 days	0.0001	M0 and M25; M75 and M100
	Age	0 % fine RCA	0.0007	7, 28 and 90 days
		25 % fine RCA	0.0003	7, 28 and 90 days
		50 % fine RCA	0.0001	7, 28 and 90 days
		75 % fine RCA	0.0002	7, 28 and 90 days
		100 % fine RCA	0.0001	28 and 90 days
Splitting tensile strength	Fine RCA percentage	Age of 7 days	0.0017	M0 and M25; M50, M75 and M100
		Age of 28 days	0.0233	M75 and M100
		Age of 90 days	0.0282	M75 and M100
	Age	0 % fine RCA	0.0370	None
		25 % fine RCA	0.0230	None
		50 % fine RCA	0.0239	28 and 90 days
		75 % fine RCA	0.0351	7 and 28 days
		100 % fine RCA	0.0349	28 and 90 days
Flexural strength	Fine RCA percentage	Age of 7 days	0.0173	M25 and M50; M75 and M100
		Age of 28 days	0.038	M0, M25 and M50; M75 and M100
		Age of 90 days	0.017	M0 and M25
	Age	0 % fine RCA	0.0001	28 and 90 days
		25 % fine RCA	0.0004	28 and 90 days
		50 % fine RCA	0.0001	28 and 90 days
		75 % fine RCA	0.0003	7, 28 days and 90 days
		100 % fine RCA	0.0015	7 and 28 days
Static modulus of elasticity	Fine RCA percentage	Age of 7 days	0.0002	M75 and M100
		Age of 28 days	0.0001	M0 y M25; M75 y M100
		Age of 90 days	0.0002	M0 y M25; M75 y M100
	Age	0 % fine RCA	0.0260	28 and 90 days
		25 % fine RCA	0.0173	28 and 90 days
		50 % fine RCA	0.0104	28 and 90 days
		75 % fine RCA	0.0256	7, 28 and 90 days
		100 % fine RCA	0.0394	7, 28 and 90 days
Poisson coefficient	Fine RCA percentage	Age of 7 days	0.0083	M25 and M50
		Age of 28 days	0.0158	M0 and M25
		Age of 90 days	0.0118	M0 and M25
	Age	0 % fine RCA	0.0285	None
		25 % fine RCA	0.0327	None
		50 % fine RCA	0.0211	None
		75 % fine RCA	0.0441	28 and 90 days
		100 % fine RCA	0.0303	None
Dynamic modulus of elasticity through the UPV	Fine RCA percentage	Age of 7 days	0.0023	M25 and M50; M75 and M100
		Age of 28 days	0.0016	M75 and M100
		Age of 90 days	0.0010	M0 y M25; M75 y M100
	Age	0 % fine RCA	0.0344	28 and 90 days
		25 % fine RCA	0.0465	None
		50 % fine RCA	0.0351	28 and 90 days
		75 % fine RCA	0.0222	28 and 90 days
		100 % fine RCA	0.0455	7, 28 and 90 days
Abrasion resistance	Fine RCA percentage	Age of 90 days	0.0043	M0, M25 and M50; M75 and M100

530

Table 10. One-way ANOVA of mechanical properties

531

4.2.9. SEM analysis

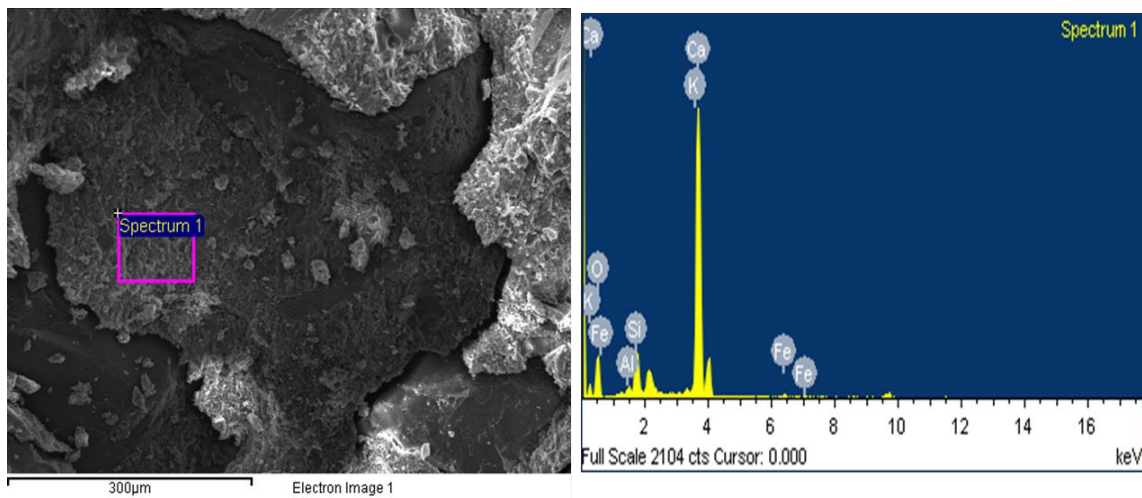
532

As commented in the introduction, the presence of adhered mortar in the RCA leads to the formation

533

of an ITZ that is less dense and of poorer quality than the ITZ between the NA and the cementitious

534 matrix [22; 25], as may be observed in the image of Figure 21, obtained from a low-strength M75 test
 535 specimen. In this image, two particles of siliceous aggregate of the RCA can be seen in both the lower
 536 right and left-hand-side corners; the old cementitious matrix (mortar adhered to the NA) of a darker
 537 color in the central part, corroborated by the microanalysis spectrum; and, the new cementitious
 538 matrix of a lighter color on the right-hand side and towards the upper right-hand-side corner. It is clear
 539 that the ITZ has failed due to its poor quality; the new cement paste shows low adhesion to the RCA,
 540 both with the mortar phase and the siliceous aggregate phase. This poor behavior of the ITZ, when
 541 adding large quantities of fine RCA, explained the variable behavior of the mixtures with high contents
 542 of fine RCA, especially in relation to the splitting tensile strength and the flexural strength.



543
 544 Figure 21. SEM analysis of mix SA75

545 **5. Conclusions**

546 In this study, the physical and mechanical behavior, at different curing ages, of a Self-Compacting
 547 Concrete (SCC) manufactured with coarse and fine Recycled Concrete Aggregate (RCA) has been
 548 studied. A preliminary statistical analysis showed an acceptable mechanical behavior of the concretes
 549 manufactured with 100 % of coarse RCA. Therefore, SCCs with 100 % RCA in the coarse fraction and
 550 different percentages (0 %, 25 %, 50 %, 75 % and 100 %) of fine RCA in substitution of Natural Aggregate
 551 (NA), 0/4 mm, were performed. The conclusions relating to the effect of the incorporation of fine RCA
 552 on these recycled SSCs are set out below:

- 553 • Increasing the mix water according to RCA water absorption was insufficient to maintain the
 554 flowability of the SCC manufactured with NA 0/4 mm when fine RCA was added. Instead, the
 555 effective water/cement ratio had to be increased. The increase in the fines content of the RCA,
 556 in comparison with NA, was favorable in the slump-flow test and the passing ability.

- 557 • All developed recycled SCCs had fresh property values within the limits of the EFNARC
558 recommendations [32]. SCC were obtained in slump-flow class SF2, viscosity class VS2 and VF2,
559 passage ability class PA1, and resistance to segregation class SR2.
- 560 • The mechanical properties of the SCC worsened as the percentage of fine RCA increased at all
561 ages of curing. On the one hand, fine RCA contents of 0 % and 25 % allowed to obtain
562 compressive strengths above 50 MPa (high strength concrete). On the other hand, the SCC
563 with a high content of fine RCA (75 % and 100 %) showed a worsening of their mechanical
564 properties with compressive strengths below 35 MPa. The one-way ANOVA showed that there
565 was no significant difference between the mechanical properties for mixes with fine RCA
566 percentages of 0 % and 25 %, and for 75 % and 100 %.
- 567 • The stress-strain curves showed that the mixtures with 75 and 100 % fine RCA were much
568 more deformable, with fracture strains of 3.7 ‰, 18.9 % higher than the fracture strain of the
569 mixture with 0 % fine RCA, which had a value of 3 ‰.
- 570 • In general, recycled SSCs with high fine RCA contents showed more uniform mechanical
571 properties over time than those with less fine RCA. According to one-way ANOVA, mixes with
572 0 % and 25 % of fine RCA showed the same strength and stiffness values at 28 and 90 days,
573 meanwhile mixes with 75 % and 100 % of fine RCA had the same values at 7, 28, and 90 days.
- 574 • The adjustment of the experimental values to the theoretical design values provided by the
575 regulations was different for each property and each recycled SCC. The theoretical values of
576 tensile strength were higher than the experimental values, both from the European standard
577 [34; 39; 42] and the ACI regulations [38], a fit that was improved by increasing the fine RCA
578 content. The theoretical modulus of elasticity, calculated with both the European and the USA
579 standard, underestimated the experimental value in mixtures with up to 25 % fine RCA, while
580 the modulus of elasticity was overestimated by percentages greater than 75 %.
- 581 • Indirect measurements, such as the Ultrasonic Pulse Velocity (UPV) and the hammer rebound
582 index yielded accurate compressive strength estimates for the concretes under analysis, with
583 the most linear adjustment for the mixtures with low contents of fine RCA. The best statistical
584 adjustment was obtained for the mixture with 100 % fine and coarse RCA.

585 In view of the above, SCC of optimum flowability and with adequate mechanical behavior can be
586 produced using high RCA contents in such a way that the SCC is valid for use in structural components.
587 In the present study, the combination of 100 % coarse RCA and a 50 % fine RCA was the limit value,
588 after which a notable worsening of the mechanical properties ensued, suggesting that the use of a fine
589 RCA content higher than 50 % in structural concretes would not be advisable in structural applications
590 from a mechanical point of view. Nevertheless, when service requirements are considered, the higher

591 deformability of the SCC due to higher fine RCA contents, shown in the stress-strain curves, is a good
592 reason for limiting the content of fine RCA to 25 %.

593 **Acknowledgements**

594 The authors wish to express their gratitude to: the Spanish Ministry MCI, AEI, EU and ERDF [grant
595 numbers PID2019-106635RB-I00; 10.13039/501100011033; FPU17/03374]; the Junta de Castilla y
596 León (Regional Government) and ERDF [grant numbers UIC-231, BU119P17]; Youth Employment
597 Initiative (JCyL) and ESF [grant number UBU05B_1274]; and finally, the University of Burgos [grant
598 numbers SUCONS, Y135.GI].

599 **Conflict of interest**

600 The authors declare that there is no conflict of interest

601 **References**

602 [1] ANEFA, ANEFHOP, ASEFMA, Informes de situación económica sectorial. Sectorial economic
603 progress reports, (2018)

604 [2] M. Sandanayake, G. Zhang, S. Setunge, Estimation of environmental emissions and impacts of
605 building construction – A decision making tool for contractors, J. Build. Eng. 21 (2019) 173-185.
606 <https://doi.org/10.1016/j.jobe.2018.10.023>

607 [3] Eurostat, Waste statistics, (2017)

608 [4] J.I. Tertre, Construction and Demolition Waste (CDW), Conference Paper, Congreso Nacional del
609 Medio Ambiente, CONAMA2016 (2016)

610 [5] M. Behera, S.K. Bhattacharyya, A.K. Minocha, R. Deoliya, S. Maiti, Recycled aggregate from C&D
611 waste & its use in concrete - A breakthrough towards sustainability in construction sector: A review,
612 Constr. Build. Mater. 68 (2014) 501-516. <https://doi.org/10.1016/j.conbuildmat.2014.07.003>

613 [6] C. Shi, Y. Li, J. Zhang, W. Li, L. Chong, Z. Xie, Performance enhancement of recycled concrete
614 aggregate - A review, J. Clean. Prod. 112 (2016) 466-472.
615 <https://doi.org/10.1016/j.jclepro.2015.08.057>

616 [7] A. Gonzalez-Corominas, M. Etxeberria, Effects of using recycled concrete aggregates on the
617 shrinkage of high performance concrete, Constr. Build. Mater. 115 (2016) 32-41.
618 <https://doi.org/10.1016/j.conbuildmat.2016.04.031>

619 [8] V. Ortega-López, J.A. Fuente-Alonso, A. Santamaría, J.T. San-José, Á. Aragón, Durability studies on
620 fiber-reinforced EAF slag concrete for pavements, Constr. Build. Mater. 163 (2018) 471-481.
621 <https://doi.org/10.1016/j.conbuildmat.2017.12.121>

622 [9] M. Skaf, E. Pasquini, V. Revilla-Cuesta, V. Ortega-López, 2019. Performance and durability of porous
623 asphalt mixtures manufactured exclusively with electric steel slags. *Materials*. 12, 3306.
624 <https://doi.org/10.3390/ma12203306>

625 [10] A.S. Brand, J.R. Roesler, Steel furnace slag aggregate expansion and hardened concrete properties,
626 *Cem. Concr. Compos.* 60 (2015) 1-9. <https://doi.org/10.1016/j.cemconcomp.2015.04.006>

627 [11] C. Pellegrino, F. Faleschini, Experimental behavior of reinforced concrete beams with electric arc
628 furnace slag as recycled aggregate, *ACI Mater. J.* 110 (2013) 197-205.

629 [12] H. Qasrawi, The use of steel slag aggregate to enhance the mechanical properties of recycled
630 aggregate concrete and retain the environment, *Constr. Build. Mater.* 54 (2014) 298-304.
631 <https://doi.org/10.1016/j.conbuildmat.2013.12.063>

632 [13] A.R. Khan, S. Fareed, M.S. Khan, Use of recycled concrete aggregates in structural concrete,
633 *Sustain. Constr. Mater. Technol.* 2 (2019)

634 [14] B. Fronek, P. Bosela, N. Delatte, Steel slag aggregate used in portland cement concrete, *Transp.*
635 *Res. Rec.* (2012) 37-42. <https://doi.org/10.3141/2267-06>

636 [15] A. Santamaria, F. Faleschini, G. Giacomello, K. Brunelli, J.T. San José, C. Pellegrino, M. Pasetto,
637 Dimensional stability of electric arc furnace slag in civil engineering applications, *J. Clean. Prod.* 205
638 (2018) 599-609. <https://doi.org/10.1016/j.jclepro.2018.09.122>

639 [16] I.Z. Yildirim, M. Prezzi, 2011. Chemical, mineralogical, and morphological properties of steel slag,
640 *Adv. Civ. Eng.* 463638. <https://doi.org/10.1155/2011/463638>

641 [17] V.W.Y. Tam, M. Soomro, A.C.J. Evangelista, A review of recycled aggregate in concrete applications
642 (2000–2017), *Constr. Build. Mater.* 172 (2018) 272-292.
643 <https://doi.org/10.1016/j.conbuildmat.2018.03.240>

644 [18] C. Thomas, J. Setién, J.A. Polanco, A.I. Cimentada, C. Medina, Influence of curing conditions on
645 recycled aggregate concrete, *Constr. Build. Mater.* 172 (2018) 618-625.
646 <https://doi.org/10.1016/j.conbuildmat.2018.04.009>

647 [19] L. Evangelista, J. De Brito, Concrete with fine recycled aggregates: A review, *Eur. J. Environ. Civ.*
648 *Eng.* 18 (2014) 129-172. <https://doi.org/10.1080/19648189.2013.851038>

649 [20] S. Santos, P.R. da Silva, J. de Brito, Self-compacting concrete with recycled aggregates – A literature
650 review, *J. Build. Eng.* 22 (2019) 349-371. <https://doi.org/10.1016/j.job.2019.01.001>

651 [21] A.M. Matos, L. Maia, S. Nunes, P. Milheiro-Oliveira, Design of self-compacting high-performance
652 concrete: Study of mortar phase, *Constr. Build. Mater.* 167 (2018) 617-630.
653 <https://doi.org/10.1016/j.conbuildmat.2018.02.053>

654 [22] S. Nagataki, A. Gokce, T. Saeki, M. Hisada, Assessment of recycling process induced damage
655 sensitivity of recycled concrete aggregates, *Cem. Concr. Res.* 34 (2004) 965-971.
656 <https://doi.org/10.1016/j.cemconres.2003.11.008>

657 [23] V.W.Y. Tam, K. Wang, C.M. Tam, Assessing relationships among properties of demolished
658 concrete, recycled aggregate and recycled aggregate concrete using regression analysis, *J. Hazard.*
659 *Mater.* 152 (2008) 703-714. <https://doi.org/10.1016/j.jhazmat.2007.07.061>

660 [24] J.T. San-José, J.M. Manso, Fiber-reinforced polymer bars embedded in a resin concrete: Study of
661 both materials and their bond behavior, *Polym. Compos.* 27 (2006) 315-322.
662 <https://doi.org/10.1002/pc.20188>

663 [25] K.P. Verian, W. Ashraf, Y. Cao, Properties of recycled concrete aggregate and their influence in
664 new concrete production, *Resour. Conserv. Recycl.* 133 (2018) 30-49.
665 <https://doi.org/10.1016/j.resconrec.2018.02.005>

666 [26] A. Yacoub, A. Djerbi, T. Fen-Chong, Water absorption in recycled sand: New experimental methods
667 to estimate the water saturation degree and kinetic filling during mortar mixing, *Constr. Build. Mater.*
668 158 (2018) 464-471. <https://doi.org/10.1016/j.conbuildmat.2017.10.023>

669 [27] V. Revilla-Cuesta, M. Skaf, F. Faleschini, J.M. Manso, V. Ortega-López, 2020. Self-compacting
670 concrete manufactured with recycled concrete aggregate: An overview. *J Clean Prod* 262, 121362.
671 <https://doi.org/10.1016/j.jclepro.2020.121362>

672 [28] M. Kazemi, R. Madandoust, J. de Brito, Compressive strength assessment of recycled aggregate
673 concrete using Schmidt rebound hammer and core testing, *Constr. Build. Mater.* 224 (2019) 630-638.
674 <https://doi.org/10.1016/j.conbuildmat.2019.07.110>

675 [29] B.B. Mukharjee, S.V. Barai, Influence of Nano-Silica on the properties of recycled aggregate
676 concrete, *Constr. Build. Mater.* 55 (2014) 29-37. <https://doi.org/10.1016/j.conbuildmat.2014.01.003>

677 [30] R. Latif Al-Mufti, A.N. Fried, The early age non-destructive testing of concrete made with recycled
678 concrete aggregate, *Constr. Build. Mater.* 37 (2012) 379-386.
679 <https://doi.org/10.1016/j.conbuildmat.2012.07.058>

680 [31] M.C.S. Nepomuceno, L.F.A. Bernardo, 2019. Evaluation of self-compacting concrete strength with
681 non-destructive tests for concrete structures. *Appl. Sci.* 9, 5109. (2019)
682 <https://doi.org/10.3390/app9235109>

683 [32] EFNARC, Specification Guidelines for Self-compacting Concrete, European Federation of National
684 Associations Representing producers and applicators of specialist building products for Concrete,
685 (2002)

686 [33] F. Fiol, C. Thomas, C. Muñoz, V. Ortega-López, J.M. Manso, The influence of recycled aggregates
687 from precast elements on the mechanical properties of structural self-compacting concrete, *Constr.*
688 *Build. Mater.* 182 (2018) 309-323. <https://doi.org/10.1016/j.conbuildmat.2018.06.132>

689 [34] EHE-08, Instrucción de Hormigón Estructural. Structural Concrete Regulations, Ministerio de
690 Fomento, Gobierno de España (2010)

691 [35] EN-Euronorm, Rue de stassart, 36. Belgium-1050 Brussels, European Committee for
692 Standardization.,

693 [36] S.C. Kou, C.S. Poon, Properties of self-compacting concrete prepared with coarse and fine recycled
694 concrete aggregates, *Cem. Concr. Compos.* 31 (2009) 622-627.
695 <https://doi.org/10.1016/j.cemconcomp.2009.06.005>

696 [37] S.A. Santos, P.R. da Silva, J. de Brito, 2017. Mechanical performance evaluation of self-compacting
697 concrete with fine and coarse recycled aggregates from the precast industry. *Materials* 10, 904.
698 <https://doi.org/10.3390/ma10080904>

699 [38] ACI-318-19, Building Code Requirements for Structural Concrete, (2019)

700 [39] EC-2, Eurocode 2: Design of concrete structures. Part 1-1: General rules and rules for buildings,
701 CEN (European Committee for Standardization) (2010)

702 [40] E. Güneş, M. Gesoğlu, Z. Algin, H. Yazici, Effect of surface treatment methods on the properties
703 of self-compacting concrete with recycled aggregates, *Constr. Build. Mater.* 64 (2014) 172-183.
704 <https://doi.org/10.1016/j.conbuildmat.2014.04.090>

705 [41] I. González-Taboada, B. González-Fonteboa, J. Eiras-López, G. Rojo-López, Tools for the study of
706 self-compacting recycled concrete fresh behaviour: Workability and rheology, *J. Clean. Prod.* 156
707 (2017) 1-18. <https://doi.org/10.1016/j.jclepro.2017.04.045>

708 [42] CEB-FIP, Model Code 2010 (Volumes 1 and 2), (2012)

709 [43] D. Carro-López, B. González-Fonteboa, J. De Brito, F. Martínez-Abella, I. González-Taboada, P.
710 Silva, Study of the rheology of self-compacting concrete with fine recycled concrete aggregates, *Constr.*
711 *Build. Mater.* 96 (2015) 491-501. <https://doi.org/10.1016/j.conbuildmat.2015.08.091>

712 [44] O. Kebaili, M. Mouret, N. Arabia, F. Cassagnabere, Adverse effect of the mass substitution of
713 natural aggregates by air-dried recycled concrete aggregates on the self-compacting ability of
714 concrete: Evidence and analysis through an example, *J. Clean. Prod.* 87 (2015) 752-761.
715 <https://doi.org/10.1016/j.jclepro.2014.10.077>

716 [45] Z.J. Grdic, G.A. Toplicic-Curcic, I.M. Despotovic, N.S. Ristic, Properties of self-compacting concrete
717 prepared with coarse recycled concrete aggregate, *Constr. Build. Mater.* 24 (2010) 1129-1133.
718 <https://doi.org/10.1016/j.conbuildmat.2009.12.029>

719 [46] S. Manzi, C. Mazzotti, M.C. Bignozzi, Self-compacting concrete with recycled concrete aggregate:
720 Study of the long-term properties, *Constr. Build. Mater.* 157 (2017) 582-590.
721 <https://doi.org/10.1016/j.conbuildmat.2017.09.129>

722 [47] T. Uygunoğlu, I.B. Topçu, A.G. Çelik, Use of waste marble and recycled aggregates in self-
723 compacting concrete for environmental sustainability, *J. Clean. Prod.* 84 (2014) 691-700.
724 <https://doi.org/10.1016/j.jclepro.2014.06.019>

725 [48] L.A. Pereira-De-Oliveira, M.C.S. Nepomuceno, J.P. Castro-Gomes, M.F.C. Vila, Permeability
726 properties of self-Compacting concrete with coarse recycled aggregates, *Constr. Build. Mater.* 51
727 (2014) 113-120. <https://doi.org/10.1016/j.conbuildmat.2013.10.061>

728 [49] R.V. Silva, J. De Brito, R.K. Dhir, The influence of the use of recycled aggregates on the compressive
729 strength of concrete: A review, *Eur. J. Environ. Civ. Eng.* 19 (2015) 825-849.
730 <https://doi.org/10.1080/19648189.2014.974831>

731 [50] P. Revathi, R.S. Selvi, S.S. Velin, Investigations on Fresh and Hardened Properties of Recycled
732 Aggregate Self Compacting Concrete, *J. Inst. Eng. Ser. A* 94 (2013) 179-185.
733 <https://doi.org/10.1007/s40030-014-0051-5>

734 [51] M. Gesoglu, E. Güneyisi, H.Ö. Öz, I. Taha, M.T. Yasemin, Failure characteristics of self-compacting
735 concretes made with recycled aggregates, *Constr. Build. Mater.* 98 (2015) 334-344.
736 <https://doi.org/10.1016/j.conbuildmat.2015.08.036>

737 [52] D.B. Lad, S.A. Faroz, S. Ghosh, 2020. Fusion of Rebound Number and Ultrasonic Pulse Velocity Data
738 for Evaluating the Concrete Strength Using Bayesian Updating, in: Varde, P.V., Prakash, R.V., Vinod, G.
739 (Eds.), *International Conference on Reliability, Safety and Hazard, ICRESH 2019*. Springer, pp. 437-448.

740 [53] B.M. Vinay Kumar, H. Ananthan, K.V.A. Balaji, Experimental studies on utilization of coarse and
741 finer fractions of recycled concrete aggregates in self compacting concrete mixes, *J. Build. Eng.* 9 (2017)
742 100-108. <https://doi.org/10.1016/j.jobe.2016.11.013>

743 [54] F. Aslani, G. Ma, D.L. Yim Wan, G. Muselin, Development of high-performance self-compacting
744 concrete using waste recycled concrete aggregates and rubber granules, *J. Clean. Prod.* 182 (2018)
745 553-566. <https://doi.org/10.1016/j.jclepro.2018.02.074>

746 [55] J.A. Ortiz, A. de la Fuente, F. Mena Sebastia, I. Segura, A. Aguado, Steel-fibre-reinforced self-
747 compacting concrete with 100% recycled mixed aggregates suitable for structural applications, *Constr.*
748 *Build. Mater.* 156 (2017) 230-241. <https://doi.org/10.1016/j.conbuildmat.2017.08.188>

749 [56] J. Xie, W. Chen, J. Wang, C. Fang, B. Zhang, F. Liu, Coupling effects of recycled aggregate and
750 GGBS/metakaolin on physicochemical properties of geopolymer concrete, *Constr. Build. Mater.* 226
751 (2019) 345-359. <https://doi.org/10.1016/j.conbuildmat.2019.07.311>

752 [57] B. Wu, H. Jin, Compressive fatigue behavior of compound concrete containing demolished
753 concrete lumps, *Constr. Build. Mater.* 210 (2019) 140-156.
754 <https://doi.org/10.1016/j.conbuildmat.2019.03.188>

755 [58] C. Zhou, Z. Chen, Mechanical properties of recycled concrete made with different types of coarse
756 aggregate, *Constr. Build. Mater.* 134 (2017) 497-506.
757 <https://doi.org/10.1016/j.conbuildmat.2016.12.163>

758 [59] F. Aslani, S. Nejadi, Mechanical characteristics of self-compacting concrete with and without
759 fibres, *Mag. Concr. Res.* 65 (2013) 608-622. <https://doi.org/10.1680/mac.12.00153>

760 [60] Y. Chen, Z. Chen, J. Xu, E.M. Lui, B. Wu, 2019. Performance evaluation of recycled aggregate
761 concrete under multiaxial compression. *Constr. Build. Mater.* 229, 116935.
762 <https://doi.org/10.1016/j.conbuildmat.2019.116935>

763 [61] L.A. Pereira-de Oliveira, M. Nepomuceno, M. Rangel, An eco-friendly self-compacting concrete
764 with recycled coarse aggregates, *Inf Constr.* 65 (2013) 31-41. <https://doi.org/10.3989/ic.11.138>

765 [62] M.K. Ismail, A.A.A. Hassan, Abrasion and impact resistance of concrete before and after exposure
766 to freezing and thawing cycles, *Constr. Build. Mater.* 215 (2019) 849-861.
767 <https://doi.org/10.1016/j.conbuildmat.2019.04.206>

768 [63] D. Pedro, J. de Brito, L. Evangelista, Structural concrete with simultaneous incorporation of fine
769 and coarse recycled concrete aggregates: Mechanical, durability and long-term properties, *Constr.*
770 *Build. Mater.* 154 (2017) 294-309. <https://doi.org/10.1016/j.conbuildmat.2017.07.215>

771 [64] G. Duarte, M. Bravo, J. de Brito, J. Nobre, Mechanical performance of shotcrete produced with
772 recycled coarse aggregates from concrete, *Constr. Build. Mater.* 210 (2019) 696-708.
773 <https://doi.org/10.1016/j.conbuildmat.2019.03.156>